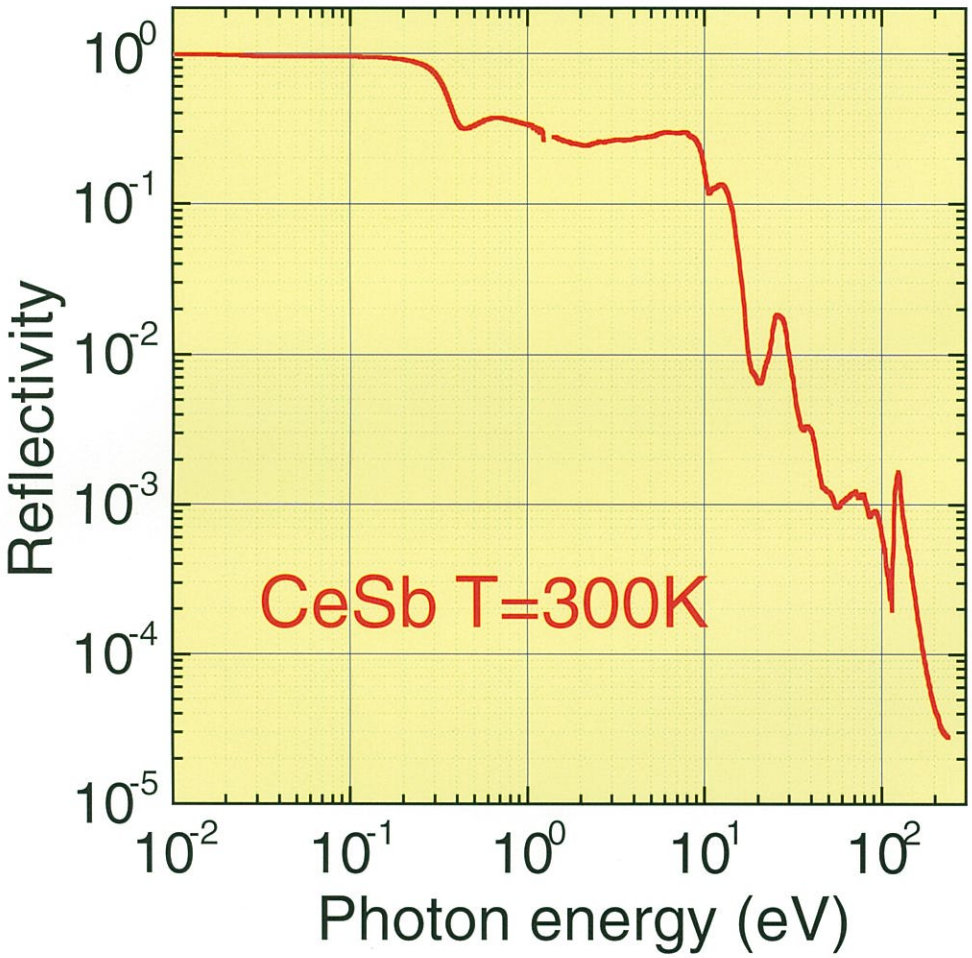

Solid State Spectroscopy I

(IR, VUV etc.)
BL1B, 3A1, 6A1, 7A, 7B

(BL1B)

Observation of new excitation channel of Cerium ion through LiCAF host crystal

Toshimasa KOZEKI, Masahiro SAKAI, Hideyuki OHTAKE, and Nobuhiko SARUKURA
Institute for Molecular Science (IMS), Myodaiji, Okazaki 444-8585, Japan
Tel: +81 564 55 7477, Fax: +81 564 55 7218, e-mail: sakai@ims.ac.jp

Zhenlin LIU, Kiyoshi SHIMAMURA, Kenji NAKANO, Na MUJILATU, and Tsuguo FUKUDA
Institute for Materials Research, Tohoku University, Katahira 2-1-1, Aoba-ku, Sendai 980-8577, Japan

Ce^{3+}:$LiCaAlF_4$ (Ce:LiCAF) [1] is already known as practical tunable ultraviolet laser crystal pumped with the fourth harmonic of an Nd:YAG laser. 60 mJ output from this laser medium was already demonstrated with large-sized CZ-grown crystal [2]. If other pumping schemes were available, it would expand the applicability of this laser medium. In this paper, we report on the observation of new excitation channel of Ce^{3+} through LiCAF host crystal.

The transmission, luminescence and excitation characteristics of Ce:LiCAF crystal were measured using Ultraviolet Synchrotron Orbital Radiation Facility (UVSOR) using 1-m focal length Seya-Namioka monochrometer with a photomultiplier. It was already known that the luminescence spectrum of Ce:LiCAF is around 290 nm. Therefore we measured the excitation characteristics of Ce:LiCAF with observation wavelength 290 nm through band-pass filters as shown in Fig.1. The two peaks in the excitation spectrum corresponded to the absorption of Ce ions. Moreover new excitation channel at around 112 nm was found. The transmission edge of the crystal is known to be about 112 nm. That is completely coincided with the peak of excitation spectrum. Therefore, this excitation can be considered as electron transfer from host crystal to the active Ce ions.

In conclusion, new excitation channel of Ce^{3+} through LiCAF host crystal was discovered. It is interesting that this excitation channel indicate the bandgap of the crystal. This excitation channel will be used as potential pumping channel.

The authors are grateful to Mr. M. Hasumoto, Dr. T. Gejo, and Prof. K. Kamada for their experimental support and stimulated discussion.

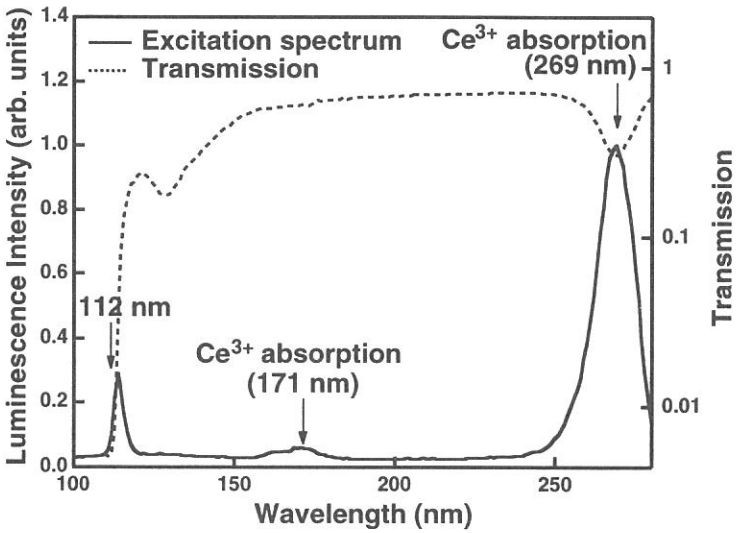

Fig.1 The excitation spectrum and transmission curve for the Ce:LiCAF crystal. The transmission edge 112 nm corresponded to the peak of excitation spectrum.

[1] N. Sarukura, Z. Liu, H. Ohtake, Y. Segawa, M. A. Dubinskii, R. Y. Abdulsabirov, S. L. Korableva, A. K. Naumov, and V. V. Semashko, "Ultraviolet short pulses from an all-solid-state Ce:LiCAF master oscillator and power amplifier system," Opt. Lett. **22**, 994-996 (1997).

[2] Z. Liu, S. Izumida, H. Ohtake, N. Sarukura, K. Shimamura, N. Mujilatu, S. L. Baldochi, and T. Fukuda, "High-pulse-energy, all-solid-state, ultraviolet laser oscillator using large Czochralski-grown Ce:LiCAF crystal," Jpn. J. Appl. Phys. **37**, L1318-L1319 (1998).

(BL1B)

Reflectance Modulation Spectroscopy of Semiconductors by Using Synchrotron Radiation and Laser

Osamu ARIMOTO, Shigeo UMEMOTO, Junpei AZUMA[A], Syuji ASAKA[B,*], Mieko SAKAMOTO, Keita NAKANISHI, Michihiro HORIMOTO[C], Toru TSUJIBAYASHI[D], Masayuki WATANABE[E], Koichiro TANAKA[A], Syunsuke NAKANISHI[F], Hiroshi ITOH[F], Minoru ITOH[C] and Masao KAMADA[G]

Department of Physics, Okayama University, Okayama 700-8530
[A]*Department of Physics, Kyoto University, Kyoto 606-8502*
[B]*Equipment Development Center, Institute for Molecular Science, Okazaki 444-8585*
[C]*Department of Electrical & Electronic Engineering, Shinshu University, Nagano 380-8553*
[D]*Department of Physics, Osaka Dental University, Hirakata 573-1121*
[E]*Department of Fundamental Sciences, Kyoto University, Kyoto 606-8501*
[F]*Department of Advanced Materials Science, Kagawa University, Takamatsu 761-0396*
[G]*UVSOR Facility, Institute for Molecular Science, Okazaki 444-8585*

Combination of synchrotron radiation (SR) and laser is an attractive and promising technique for solid-state research such as two-photon spectroscopy or pump-probe experiments focused on inner-shell electronic states. We have so far investigated exciton structures in wide-gap materials BaF_2 and CaF_2, in which the luminescence induced by two-photon excitation with SR and laser is detected [1-6]. In order to ascend a new step in the combined experiments, we have developed in the present work an experimental system of reflection-type, that is, reflectivity changes induced by laser irradiation are detected in the VUV region with probe light from SR. This system will be useful and powerful especially in the cases where measurements of luminescence or absorption are difficult. Measurements for ZnSe and n-GaAs crystals have been made in order to check the suitability of our system.

In Fig. 1 is shown a schematic diagram of the experimental setup for ZnSe. A second harmonics of CW mode-locked Ti:sapphire laser (Coherent, Mira 900-F/P) was generated with a harmonic generator (Coherent, 5-140 UltraFast Harmonic Generator), and was used as an excitation light source. The synchronization of SR and laser pulses was achieved by a phase-locked loop circuit (Coherent, Mira Synchro-lock 9300), which locked the laser timing to the 90 MHz signal from the RF master oscillator. In order to enlarge the temporal overlap between the SR pulse (1.5 ns) and the laser pulse (160 fs), the laser beam was injected into a multi-mode optical fiber with length of 50 m, which stretches the pulse width to about 300 ps [6]. A ZnSe crystal with thickness of 6000 A grown onto GaAs substrate by molecular beam epitaxy was studied. The band gap energy of ZnSe is 2.82 eV, so that interband excitation was made with the laser light (3.12 eV,13 mW). A glass envelope of the photomultiplier tube (PMT) with CsI photocathode (Hamamatsu Photonics, R2032) was cut down, and it was installed into a sample chamber. Reflected light from the sample was detected with the PMT, and reflectivity change synchronized with the chopped laser light was measured with a lock-in amplifier. In luminescence-detected SR-laser combined experiments, one has to eliminate strong laser scattering light for observing weak luminescence signal. In the present system, on the other hand, the PMT of solar-blind type has no sensitivity for the laser light, so that the problem of laser scattering is cleared away. At present, the system has sensitivity of reflectivity change $\Delta R/R = 10^{-5}$.

Figure 2 shows reflectance modulation spectrum of ZnSe at 15 K. The spectrum was not measured below 6.2 eV, where the PMT does not have enough sensitivity. Significant reflectivity changes are seen in the region from 6.2 to 7.5 eV. As an origin of the reflectivity change, we first checked an effect of temperature increase of the sample due to the laser irradiation, i.e., temperature modulation of the reflectance. The temperature change induces an energy shift of the reflection spectrum. In a rough approximation, therefore, thermoreflectance is to be the same as the wavelength modulation reflectance [7]. However, the derivative of the observed reflection spectrum with respect to energy was found not to agree with the modulation spectrum observed, indicating

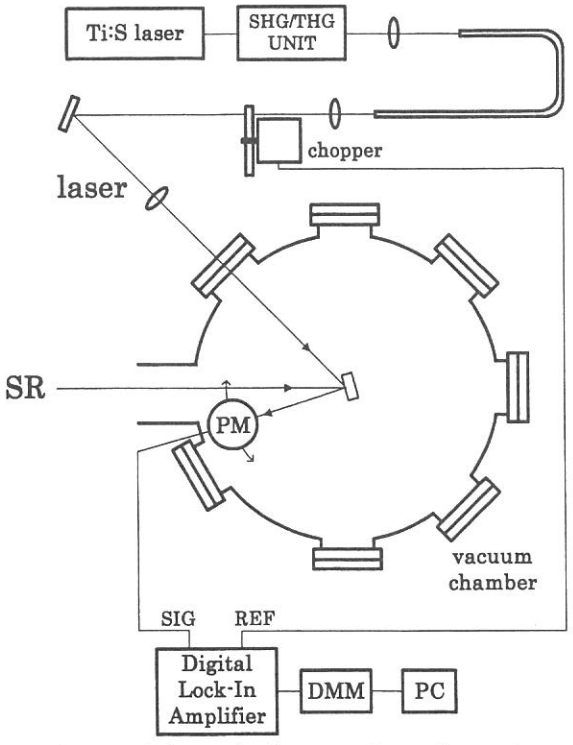

Fig. 1. Schematic diagram of experimental system for reflectance modulation.

negligible contribution of the temperature modulation in the present system.

We consider that the reflectivity change arises from an electric field modulation. The ZnSe crystal has usually an n-type conductivity, and the band bending is inherently induced in a depletion region near the surface. The electrons and holes photoexcited by laser light find themselves in that electric field, and separate spatially in a manner so as to reduce the built-in field. Consequently the reflectance is modulated by the periodic cancellation of the built-in surface field due to the free carriers created by chopped laser light, that is, the present modulation reflectance is originated from the electroreflectance. In general, electroreflectance shows the well-known Franz-Keldysh oscillation under a medium or strong electric field, which allows us identification of critical points. Under a weak electric field, on the other hand, it is shown that the $\Delta R(\omega)$ spectrum is identical with the third derivative of original spectrum $R(\omega)$ [7]. In fact, it was found that d^3R/dE^3 spectrum agrees with the observed $\Delta R(\omega)$ spectrum except an energy range from 6.8 to 7.3 eV; the d^3R/dE^3 spectrum shows no structure there. It has been reported that ZnSe shows reflectivity structures at 6.50 eV and 6.63 eV at room temperature and they are assigned to transitions at Δ_5^v- Δ_5^c and plateau near (0.8, 0.2, 0.2) in the Brillouin zone, respectively, from the band calculation [8]. The structures peaking at 6.45 and 6.62 eV in Fig. 2 are related with these transitions. It is plausible that the observed structures around 7.0 eV appear due to other transitions, which are hidden in the reflection spectrum.

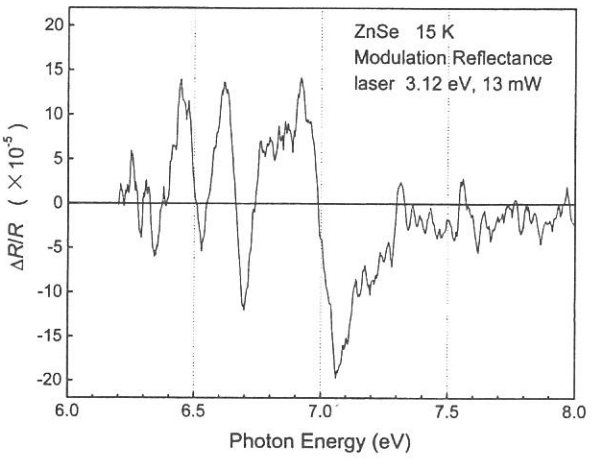

Fig. 2. Reflectance modulation spectrum of ZnSe at 15 K.

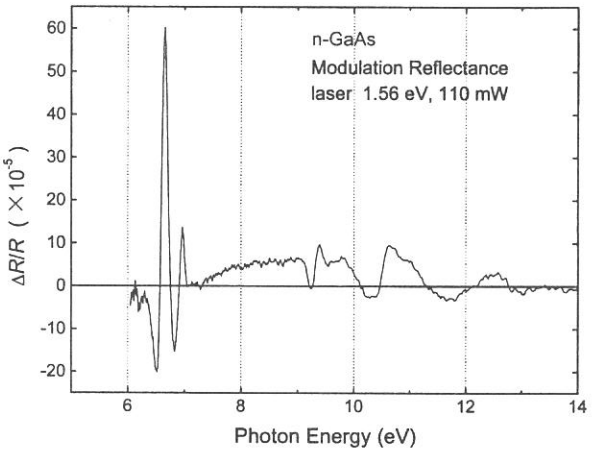

Fig. 3. Reflectance modulation spectrum of n-GaAs at 15 K.

In Fig. 3 is shown modulation reflectance spectrum of n-GaAs (band gap energy 1.520 eV, donor concentration ~10^{18} /cm^3) at 15 K. In this case, fundamental light of Ti:sapphire laser (1.56 eV, 110 mW) was used to create free carriers. An intense reflectivity change is seen at 6.6 eV. Spectral position and shape agree well with those of the electroreflectance [9], if the sign of ΔR is reversed. This fact definitely shows that the observed reflectivity change is caused by the electric field modulation mentioned above. The reverse sign indicates the quenching of the built-in surface electric field due to photocarriers.

In conclusion, we have developed the SR-laser combined experimental system of reflection-type. The system provides non-contact electric field modulation spectroscopy in VUV region without any electrodes, and will be effective for the study on dynamics of photoexcited carriers in semiconductors.

The present work was partly supported by a Grant-in-Aid for Scientific Research from the Ministry of Education, Culture, Sports, Science and Technology.

References

[1] M. Kamada *et al.*: J. Synchrotron Radiation **5** (1998) 1035.
[2] O. Arimoto: J. Electron Spectrosc. Relat. Phenom. **92** (1998) 219.
[3] S. Asaka *et al.*: Rev. Sci. Instrum. **69** (1998) 1931.
[4] T. Tsujibayashi *et al.*: Phys. Rev. B **60** (1999) R8442.
[5] T. Tsujibayashi *et al.*: J. Lumin. **87** (2000) 254.
[6] J. Azuma *et al.*: Nucl. Instrum. Methods (2001) (in press).
[7] P. Y. Yu and M. Cardona: *Fundamentals of Semiconductors* (Springer-Verlag, Berlin, 1996).
[8] J. R. Chelikowsky and M. L. Cohen: Phys. Rev. B **14** (1976) 556.
[9] D. E. Aspnes, C.G. Olson and D. W. Lynch: Phys. Rev. B **12** (1975) 2527.

* Present address: Elementary and Secondary Education Bureau, Ministry of Education, Culture, Sports, Science and Technology, Tokyo 100-0013

(BL1B)

Polarized Reflectivity Spectra of Exciton Band in $PbWO_4$

Masami FUJITA, Minoru ITOH[A], Michihiro HORIMOTO[A],
Hisanobu KUNISAKI[A] and Yoshiyuki USUKI[B]

Japan Coast Guard Academy, Wakaba, Kure 737-8512
[A] *Department of Electrical and Electronic Engineering, Faculty of Engineering, Shinshu University, Nagano 380-8553*
[B] *Materials Research Laboratory, Furukawa Co., Kannondai, Tsukuba 305-0856*

Lead tungstate ($PbWO_4$; PWO) is a well-known scintillating substance. Although the luminescence properties have been extensively studied in the application field, basic investigations on the optical constants such as reflectivity spectra have been still scarce [1-4]. The PWO has two structural modifications, scheelite (tetragonal) and raspite (monoclinic) structures. Recently we measured optical spectra of both phases [3,4]. Belsky *et al.* [1] have reported that the intensity of the exciton band of scheelite crystals is strongly affected by the stoichiometry of samples. However, if one wants to discuss the change in spectra, the polarization dependence of optical constants should be examined in detail, because the scheelite crystal has an anisotropic structure. In the present study we have measured polarized reflectivity spectra of pure and impurity-doped PWO crystals in order to reveal the optical anisotropy and the effect of impurity doping in the exciton band region.

Single crystals of undoped and impurity-doped PWO were grown by the Czochralski method. The dopants investigated here were Cd^{2+}, La^{3+}, Gd^{3+}, Y^{3+}, Th^{4+}, Nb^{5+} and Mo^{6+} ions. Reflectivity spectra were measured at 6 K on the cleaved surfaces of (011) plane [5], with the electric vector parallel ($\boldsymbol{E} \parallel \boldsymbol{a}$) and perpendicular ($\boldsymbol{E} \perp \boldsymbol{a}$) to the $\boldsymbol{a}$-axis.

Figure 1 shows reflectivity spectra of undoped PWO single crystal in the 3–7 eV region. A strong exciton band is observed for the polarization $\boldsymbol{E} \parallel \boldsymbol{a}$. The band consists of two components at 4.25 eV and 4.38 eV as reported in Refs. [3,4]. On the other hand, weak structures are observed at 4.22 eV and 4.45 eV for $\boldsymbol{E} \perp \boldsymbol{a}$. A broad peak is found at 5.27 eV for $\boldsymbol{E} \perp \boldsymbol{a}$, while it is not observed for $\boldsymbol{E} \parallel \boldsymbol{a}$. The peaks at 3.3 eV and 4.0 eV are spurious structures due to the reflection from the rear surface of the sample, because no structures are observed in the absorption spectrum shown in Fig. 1. The absorption band at 3.5 eV is likely ascribed to some lattice imperfection.

In Fig. 2 are shown reflectivity spectra of samples doped with Mo^{6+} (1350 ppm) for $\boldsymbol{E} \parallel \boldsymbol{a}$ and with La^{3+} (1350 ppm) for $\boldsymbol{E} \perp \boldsymbol{a}$. The spectral features above 4.1 eV are essentially the same as those for the corresponding polarization in Fig. 1. Similar polarized reflectivity spectra were obtained for PWO crystals doped with the other impurity ions. When the polarization of light was arbitrary chosen with respect to the crystal orientation, the spectrum exhibits a mixed character of the $\boldsymbol{E} \parallel \boldsymbol{a}$ and $\boldsymbol{E} \perp \boldsymbol{a}$ spectra, as exemplified by the spectrum of the sample doped with Cd^{2+} (1%) in Fig. 2. The humps and peaks below 4.0 eV in Fig. 2 are again due to the reflection from the rear surface of samples.

No appreciable change of the reflectivity spectrum, as well as its polarization dependence, is seen between Fig. 1 and Fig. 2, except for a small broadening of the exciton band of doped samples. This fact indicates that the electronic structures of PWO are hardly affected by the doping of various types of impurity ions.

The present result strongly suggests that the intensity variation of the exciton band pointed out by Belsky *et al.* is ascribed to the anisotropy of the transition intensity, rather than the difference in the stoichiometry of samples [1]. According to the energy band calculation of PWO [6], the valence band is formed by the 2*p* state of O^{2-} ions, and the conduction band is built up of the 5*d* state of W^{6+} ions. Furthermore, the Pb^{2+} 6*s* state hybridizes throughout the valence band, and the Pb^{2+} 6*p* state contributes to the conduction band. The dichroism of the exciton band observed in the present experiment would be ascribed to the crystal-field splitting of the Pb^{2+} 6*p* states in the axial crystal field along the *c*-axis.

The authors would like to thank Prof. M. Kobayashi (KEK) for useful comments on PWO crystals.

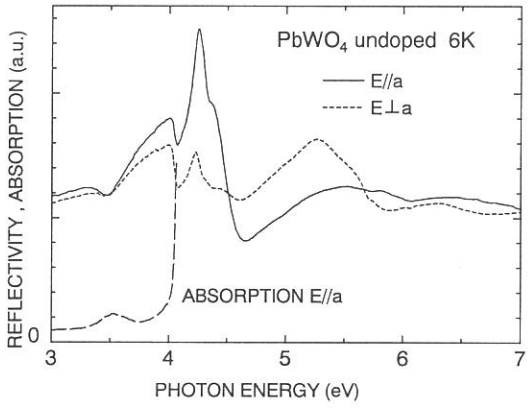

Fig. 1 Reflectivity and absorption spectra of undoped $PbWO_4$ crystal.

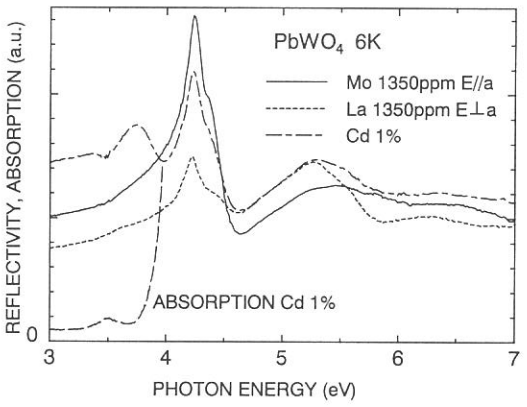

Fig. 2 Reflectivity and absorption spectra of $PbWO_4$ crystals doped with impurities.

References

[1] A. N. Belsky, S. M. Klimov, V. V. Mikhailin, A. N. Vasil'ev, E. Auffray, P. Lecoq, C. Pedrini, M. V. Korzhik, A. N. Annenkov, P. Chevallier, P. Martin and J. C. Krupa: Chem. Phys. Lett. **277** (1997) 65.

[2] I. N. Shpinkov, I. A. Kamenskikh, M. Kirm, V. N. Kolobanov, V. V. Mikhailin, A. N. Vasil'ev and G. Zimmerer: Phys. Status. Solidi (A) **170** (1998) 167.

[3] M. Itoh, D. L. Alov and M. Fujita: J. Lumin. **87-89** (2000) 1243.

[4] M. Itoh and M. Fujita: Phys. Rev. B **62** (2000) 12825.

[5] M. Ishii, K. Harada, M. Kobayashi, Y. Usuki and T. Yazawa: Nucl. Instrum. Methods Phys. Res. A **376** (1996) 203.

[6] Y. Zhang, N. A. W. Holzwarth and R. T. Williams: Phys. Rev. B **57** (1998) 12738.

(BL1B)

Optical Spectra of MoO_3 Single Crystals Investigated by Polarized Light

K. Hayakawa, M. Itoh, S. Oishi[1] and M. Fujita[2]

Department of Electrical and Electronics Engineering, Shinshu University, Nagano 380-8553

[1]Department of Environmental Science and Technology, Shinshu University, Nagano 380-8553

[2]Japan Coast Guard Academy, Wakaba, Kure 737-8512

Molybdenum trioxide (MoO_3) has been widely used as a catalyst in the chemical industry. Recently, this material is attracting attention as an optical substance from the viewpoint of technical engineering, because it has a special character such as photochromism or electrochromism. An early study of this material was performed by Deb and Chopoorian in 1966 [1]. Although there are many investigations on amorphous and thin MoO_3 films, few studies have been done for the single crystals.

Single crystals investigated in this work were grown by the sublimation method. The crucible filled with reagent-grade MoO_3 powder was heated to 780－900℃ for 5－10 hours. The temperature gradient along the crucible allowed us to grow single crystals at the relatively cooler upper edge and crucible lid. The MoO_3 crystals obtained were transparent in the visible region.

Figure 1 shows reflectivity spectra of MoO_3 measured at 6 K in the energy range between 3 and 25 eV for the polarization parallel to the *a* axis (E // a) and to the *c* axis (E // c). The absolute values of the reflectivity were not measured in the present experiment. Fortunately, the refractive indices of MoO_3 at 2.1 eV have been measured to be 2.29 for E // a and 2.54 for E // c [2]. Using these values, we obtained the reflectivity spectra of Fig. 1.

The reflectivity spectra exhibit remarkable polarization dependence. The spectrum for E // c rises at lower energy than that for E // a, as shown clearly in Fig. 2. Both spectra are structure-rich in the energy region below 12.5 eV, and have a broad structure at around 20－25 eV.

The imaginary part of the dielectric function and the absorption coefficient have been derived through the Kramers-Kronig analysis of the reflectivity spectra in Fig. 1. The obtained results are shown in Fig. 3. For E // c, three sharp bands are observed at 4.7, 6.1 and 8.6 eV. A weak peak is also seen at 10.5 eV. For E // a, one can see three sharp bands at 4.9, 8.4 and 10.0 eV. Furthermore, doublet structure peaking at 5.5 and 5.9 eV is observable.

No information on the electronic structures of MoO_3 has been available in the literature. Therefore, we calculated the electronic states of a model cluster of MoO_3 by using the DV-Xα method. The crystal structure of MoO_3 belongs to the orthorhombic type, in which molybdenum ions are connected with oxygen ions to form the chain parallel to the *c* axis. The oxygen ion in the direction of *a* axis is connected with this chain, and that in the *b* axis combines weakly with one molybdenum ion. Accordingly, the MoO_3 forms a layered structure. Because of the low symmetry of MoO_3, we used an embedded cluster model for a more accurate calculation. The oxygen ions surrounding a molybdenum ion are divided into two groups. One is the O^{2-}[I] ion aligned

along the *c* axis, and the other is the O^{2-}[II] ion along the *a* axis.

The present calculation indicates that the valence band is dominated by the 2*p* state of oxygen ions, and the lowest conduction band is mainly built up of the 4*d* state of molybdenum ions. The calculated band-gap is 3.9 eV, which is in satisfactorily agreement with the experimental result. The top of the valence band originating from O^{2-}[II] is located at 1.8 eV below that from O^{2-}[I]. This result may explain the difference between the solid and dotted curves in Fig. 2. The absorption spectra of Fig. 3 show a clear dip at around 7 eV higher than the absorption edges. Since the valence-band width is calculated to be about 7.0 eV, the structures observed below the dip are attributed to the transitions from the valence band to the bottom of the conduction band.

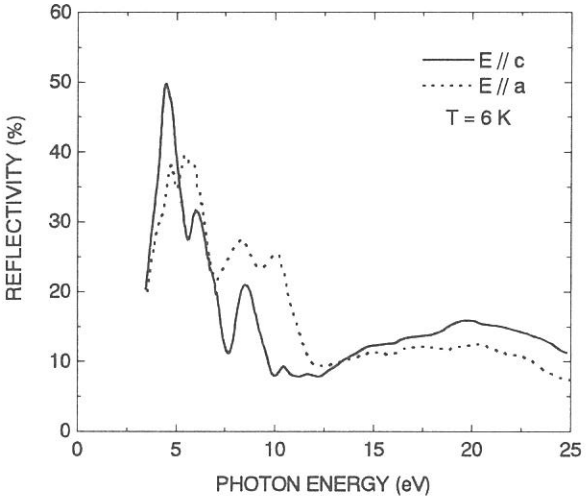

Fig. 1. Reflectivity spectra of single crystal MoO_3 (solid curve ; *E* // *c* and dotted curve; *E* // *a*) at 6 K.

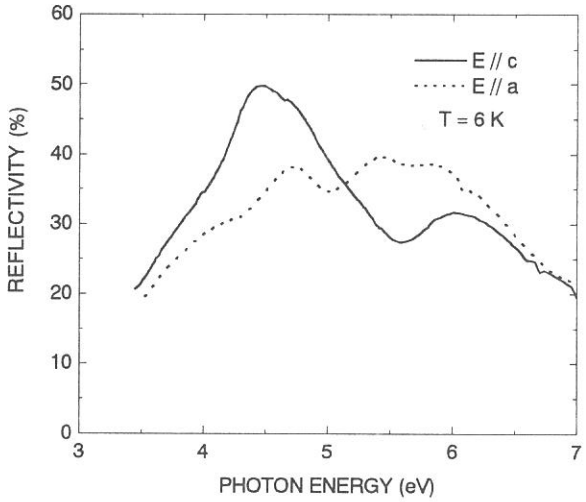

Fig. 2. Reflectivity spectra of MoO_3 in the energy region between 3 and 7 eV at 6 K.

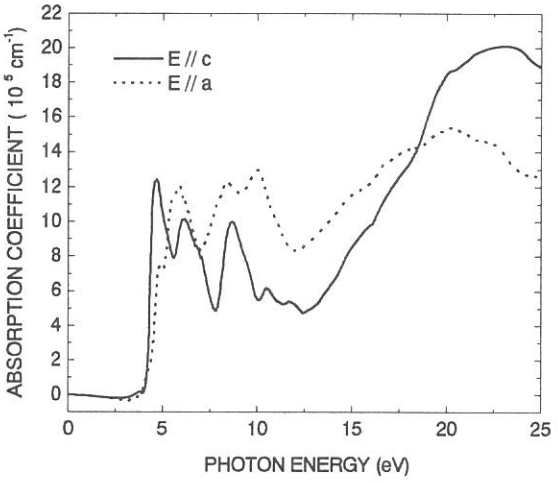

Fig. 3. Absorption spectra of MoO_3 derived through the Kramers-Kronig analysis of the reflectivity spectra in Fig. 1.

References

[1] S. K. Deb and J. A. Chopoorian: J. Appl. Phys. **37** (1966) 4818.

[2] S. K. Deb: Proc. Roy. Soc. A. **304** (1968) 211.

(BL1B)

in-situ VUV absorption spectra and emission spectra of mesoporous silica powder using quartz *in-situ* cell

Yoshitaka Inaki,[1] Hisao Yoshida,[1] Tomoko Yoshida [2] and Tadashi Hattori [1]

[1] *Department of Applied Chemistry, Graduate School of Engineering, Nagoya University, Nagoya 464-8603, Japan.*

[2] *Center for Integrated Research in Science and Engineering, Nagoya University, Nagoya 464-8603, Japan.*

Introduction

We have been studied for a several years about amorphous silica powder catalyst having high surface area (above 500 m^2 g^{-1}) and large amount of surface SiOH groups (~5 OH/nm^2). In our previous study, we discovered that pure silica materials evacuated at high temperature exhibit the photometathesis activity [1]. Metathesis reaction is known to occur only on transition metal catalyst including Mo, Re and W, and therefore, metathesis activity over silica is very unique. We expected that the active sites for photometathesis would be the strained siloxane bridges (≡Si−O⋯⋯Si≡) generated by dehydroxylation of surface isolated SiOH at high temperature such as above 673 K [1, 2]. However the strained siloxane bridges were observed only by infrared spectra and those detailed structure has not been revealed.

Vacuum UV (VUV) and UV spectroscopy is a useful tool for the observation of the defect center on the silica surface and in the bulk silica. The aim of this study is to observe the specific sites on silica materials evacuated at high temperature. In order to measure the spectra of such treated samples without exposure to air, the quartz *in-situ* cell shown in Fig. 1 was used.

Experimental

The silica powder samples we used were amorphous silica and mesoporous silica materials (FSM-16 and MCM-41). Amorphous silica was prepared by sol-gel method. FSM-16 and MCM-41 were prepared by referring the reports [2].

Fig. 1 shows the pretreatment cell. The sample in the pretreatment part (A) was performed at 1073 K in O_2 for 1h, followed by the evacuation at 1073 K for 1h by a diffusion pump (the pressure reached to 10^{-4} ~ 10^{-5} Torr). After pretreatment, the sample was transferred to the measurement part (B) made of quartz and the glass tube was sealed and cut without exposure to air. Then, measurement part was attached to the sample folder (C) by using the carbon adhesive sheet.

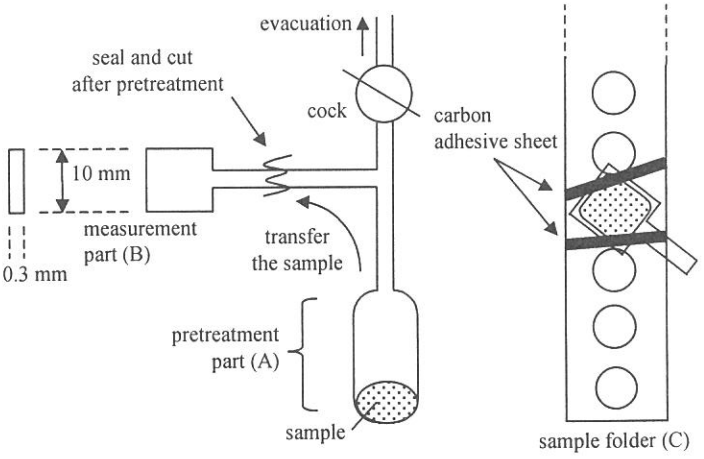

Figure 1 The pretreatment cell (left) and the attachment of sample (right).

VUV spectra and photoluminescence spectra were measured at room temperature using synchrotron radiation at the beam line 1B station (BL-1B) attached with an 1 m Seya-Namioka monochrometer at UVSOR, Institute for Molecular Science, Okazaki, Japan, operated at electron energy of 750 MeV. Photoluminescence spectra were measured by using monochrometer (Spex 270M) and photomultiplier (Hamamatsu R4220).

Results and Discussion

Fig. 2 shows the VUV spectra of FSM-16, MCM-41 and amorphous silica, evacuated at various temperatures. FSM-16 and MCM-41 showed the complex spectra (Fig. 2Aa, 2Ab), which were probably consisted of four absorption bands and the threshold at band gap of silica (8.1 eV, 153 nm) (Fig. 2B). The four bands could be assigned to the defect centers in the bulk silica and on the silica surface [3], respectively: ≡Si-Si

≡ at 7.6 eV (163 nm), ≡Si...Si≡ at 6.9 eV (180 nm), ≡Si·(E' center) at 6.1 eV (203 nm) and =Si : center ($B_2\beta$) and/or ≡Si-O· center (non-bridging oxygen hole center, NBOHC) at 4.75 eV (261 nm). On the other hand, only small absorption band was observed on amorphous silica (Fig. 2Ac), although absorption intensities could not be discussed because these were varied easily by the sample density in the *in-situ* cell. Since effective wavelength for photometathesis over silica is in UV region below ca. 370 nm (> 3.4 eV) [2], either of two defect centers at 261 nm are candidate for the photocatalytic active sites.

Fig. 3 shows the photoluminescence spectra of silica materials evacuated at 1073 K. Only on FSM-16, emission peak was observed at 390 nm (Fig. 3B), which emission was excited by the light at 250 nm (Fig. 3A). This emission band would be assigned to =Si : ($B_2\beta$ center) [3]. On the other hand, $B_2\beta$ center was not observed on MCM-41 and amorphous silica, although these were also active for photometathesis. These suggest that the $B_2\beta$ center should not be the photometathesis active sites. Probably, the another defect sites also showing the absorption band at 261 nm, i. e., ≡Si-O· (NBOHC), should be photometathesis active site rather than $B_2\beta$ center, and ≡Si-O· may relate to the strained siloxane bridges.

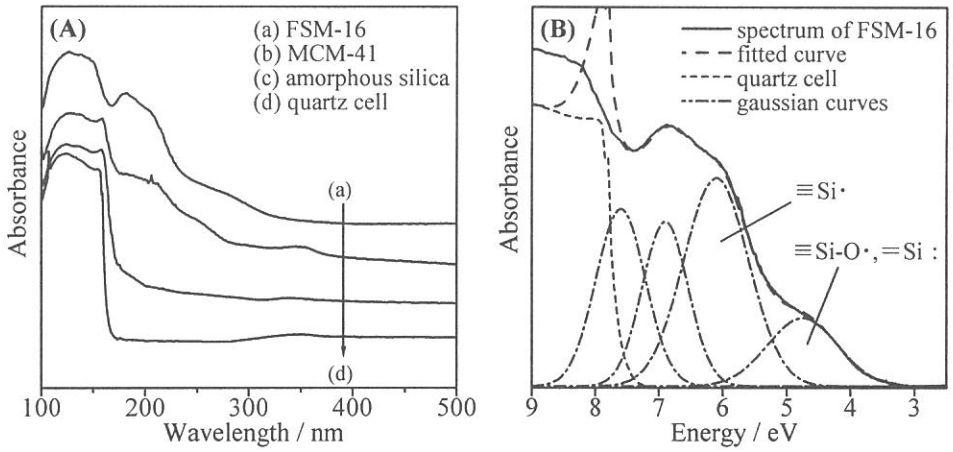

Figure 2 VUV-UV-visible spectra of silica materials evacuated at 1073 K, and of the quartz cell (A), and the spectrum of FSM-16 fitted by a curve of the quartz cell and four Gaussian curves at 7.6 eV, 6.9 eV, 6.1 eV and 4.75 eV (B). Fitting curve did not fit above 7.6 eV, because very large band of the band gap of silica existed and transmittance was extremely low.

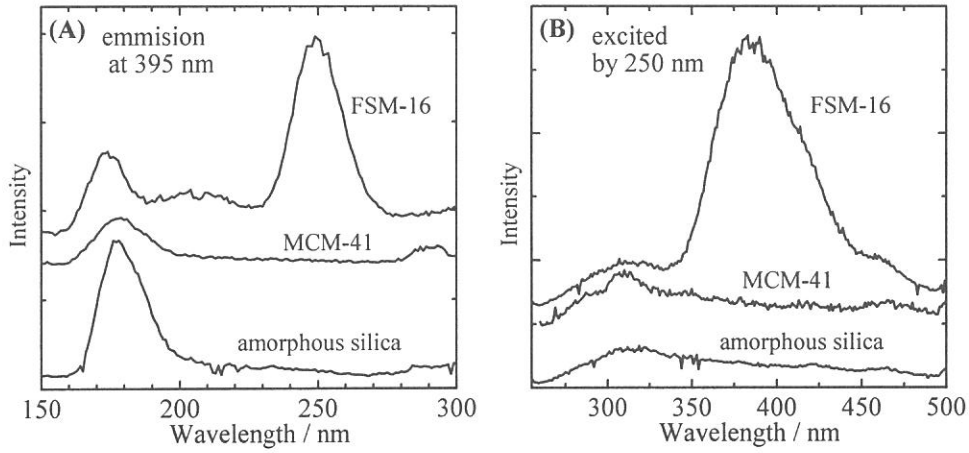

Figure 3 Photoexcitation spectra (A) and photoemission spectra (B) of silica materials evacuated at 1073 K. Peaks around at 175 nm in (A) would be emission from the lens attached to the monochrometer.

[1] Y. Inaki, H. Yoshida, K. Kimura, S. Inagaki, Y. Fukushima and T. Hattori, *Phys. Chem. Chem. Phys.* **2**, 5293 (2000).

[2] Y. Inaki, H. Yoshida and T. Hattori, *J. Phys. Chem. B* **104**, 10304 (2000).

[3] L. Skuja, *J. Non-Cryst. Solids* **239**, 16 (1998).

(BL1B)

Photoionization of Soluble Dye Molecules at the Water Surface

T. Ishioka, K. Seno, T. Sugiyama, A. Harata, and Y. Hatano

Department of Molecular and Material Sciences, Kyushu University, Kasuga-shi, Fukuoka, 816-8580, Japan

Understanding of the spectroscopy and dynamics of photoexcitation and photoionization of molecules at the liquid surface is of essential importance in fundamental and applied sciences. Since little is known such interesting behavior of molecules,[1] RhodamineB (RhB) is chosen in this study as an example of soluble molecules at the liquid water surface for photoionization experiments because of our previous studies of this molecule in laser two-photon ionization experiments.[2]

The experimental setup for photoionization is shown in Fig. 1. Synchrotron radiation obtained at BL-1B of the UVSOR was used as an excitation source. Its intensity was calibrated using a photodiode (Hamamatsu Photonics, S2281-01) for each measurement. The solution of RhB with liquid water was kept on a stainless-steel vessel and high voltage (2000 V/cm) was applied between water surface and an electron-trapping electrode settled in the vessel purged with He gas. The photoionization current was measured using a current meter (Keithley, 617).

Figure 2 shows the photon energy dependence of the photoionization current on RhB solution surface with its threshold at 5.4 eV, which is identified with the lowest photoionization threshold of RhB at the water surface. This result is consistent with the previous one.[2] In the photon energy range above 5.4 eV, the increase in the magnitude of the observed photocurrent I is observed and explained by the following empirical power law represented by

$$I = C\,(h\nu - E_{th})^{\alpha} \qquad (1)$$

with α=2.5, where C is a constant and E_{th} is the ionization threshold.[3] The change in the slope value with increasing the photon energy starting from the threshold, which is observed also in pure liquid hydrocarbons,[4] is explained by the multiple photoionization thresholds corresponding to different molecular orbitals. It is interesting to apply this explanation to the present experiment of the photoionization behavior of RhB molecules on the water surface since RhB is composed of different moieties such as xanthene structure, carboxyphenyl group, and substituted amines. At the water surface, it is also possible to account for the above result by the condition of RhB with different hydration state, depth profile from the surface, and aggregation at the surface. Further experiments are greatly needed to understand the spectroscopy and dynamics of photoexcitation and photoionization of molecules at the liquid surface as opposed to those of isolated molecules in the gas phase.[5]

References

[1] T. Inoue, S. Sasaki, M. Tokeshi, and T. Ogawa, *Chem. Lett.*,**1998**, 609.

[2] T. Ishioka, K. Seno, S. Sasaki, and A. Harata, *UVSOR Activity Report*, **1999**, 70.

[3] J. Casanovas, R. Grob, D. Delacroix, J. P. Guelfucci, and D. Blanc, *J. Phys. Chem.*, **75**, 4661 (1981).

[4] H. Koizumi, K. Lacmann, and W. F. Schmidt, *J. Elec. Spectrosc. Relat. Phenom.*, **67**, 417 (1994).

[5] Y. Hatano, *Phys. Reports*, **313**, 110 (1999).

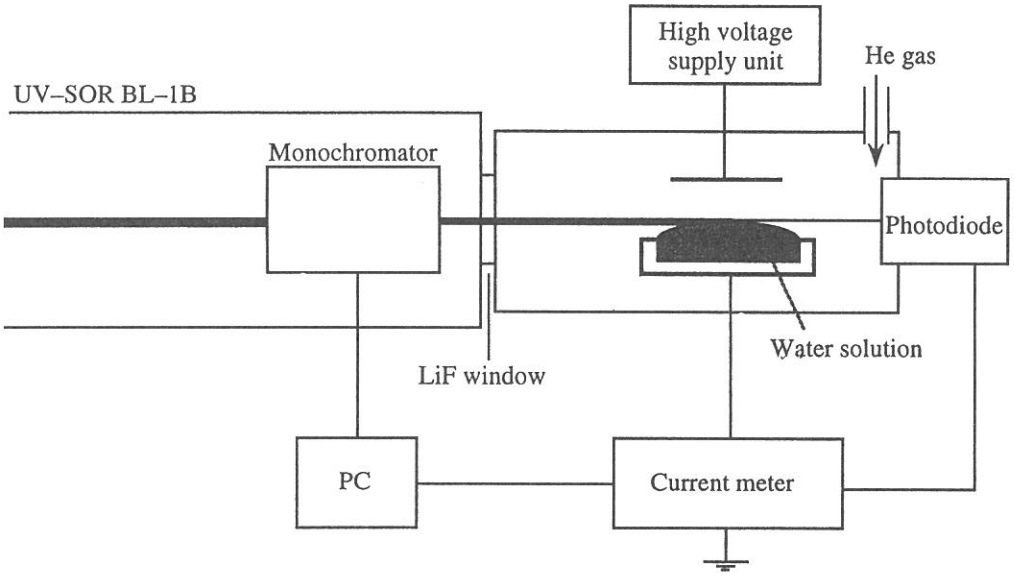

Fig. 1 Schematic diagram of the photoionization spectrometer using SR light.

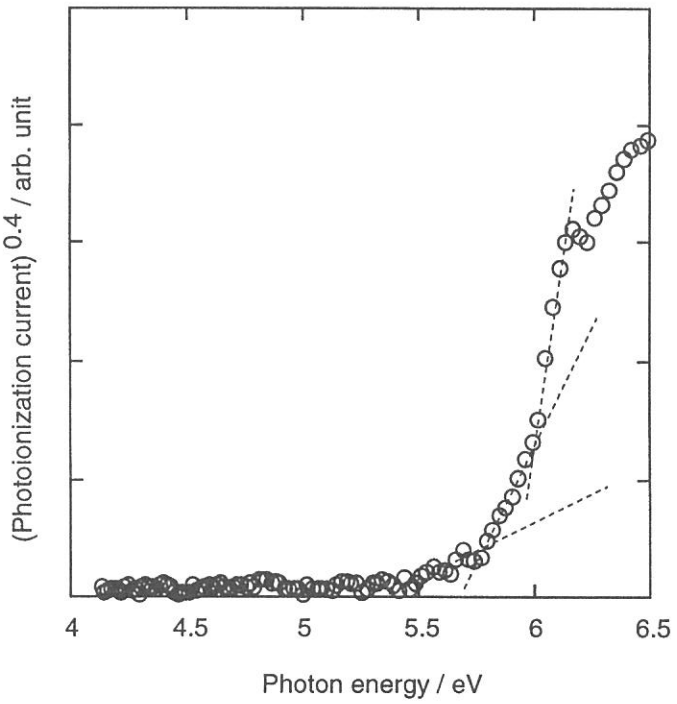

Fig. 2 Photon energy dependence of photoionization current from the surface of aqueous RhodamineB solution. The concentration of RhodamineB was 3.9 μM.

(BL1B)

Luminescence Properties of Tb^{3+} Ions in Mg_2SiO_4 Crystals

M. Kitaura[A], H. Nakagawa[B], K. Ebisu[B] and R. Mizuno[B]

[A]*Fukui National College of Technology, Sabae, 916-8507*

[B]*Department of Electrical and Electronics Engineering, Fukui University, Fukui 910-8507*

Magnesium silicate (Mg_2SiO_4) activated with Tb^{3+} ion has been studied for application in a thermoluminescence dosimeter under irradiation with VUV- light, X- ray and electrons. The thermo-luminescence is certainly induced by electron- hole recombination at the Tb^{3+} ion sites; however, the process has not yet been understood. In the present study, we have investigated luminescence properties of Tb^{3+} ions in Mg_2SiO_4 under excitation with UV- and VUV-light.

The crystals of Mg_2SiO_4:Tb were grown in air from the sintered rods by the floating zone method using an infrared imaging furnace. The concentration of Tb^{3+} ions in the crystals was weighed to 0.1 mol%. The sample was cut off from a crystal ingot, and was mounted on the copper holder of a temperature variable cryostat. The present experiments were carried out at BL1B of UVSOR, where monochromatic light from a 1-m Seya-Namioka type monochromator is available for excitation. Luminescence from the sample was detected by a combination of quartz lenses, a monochromator (Jobin-Yvon HR 320) and a photomultiplier tube (Hamamatsu R955). Excitation spectra reported here were corrected for the spectral distribution of excitation light by using sodium-salycilate phosphor.

Figure 1 shows the absorption spectrum of Mg_2SiO_4:Tb measured at 9 K. Three bands are observed at 4.57, 5.11 and 5.58 eV. These bands were not observed in pure Mg_2SiO_4. This result indicates that the incorporation of Tb^{3+} ions is responsible for the three bands. In addition, their peak energies are in agreement with those of $4f \rightarrow 5d$ bands of Tb^{3+} ions in Y_2SiO_5 [1]. Therefore, the three bands in Fig. 1 are assigned to the $4f \rightarrow 5d$ bands of Tb^{3+} ions in Mg_2SiO_4. In the high-energy side, the absorption spectrum rises drastically. Such a rise corresponds to the fundamental absorption edge of host Mg_2SiO_4. Figures 2 (a) and (b) show emission spectra of Mg_2SiO_4:Tb at 10 K. The excitation photon energy in (a) corresponds to the fundamental absorption region, and that in (b) to a $4f \rightarrow 5d$ absorption peak. In Figs. 2 (a) and (b), sharp emission bands are seen in the range of 1.7-3.5 eV. From comparison with emission spectra of Tb^{3+} ions in Y_2SiO_5 [1] and $YAlO_3$

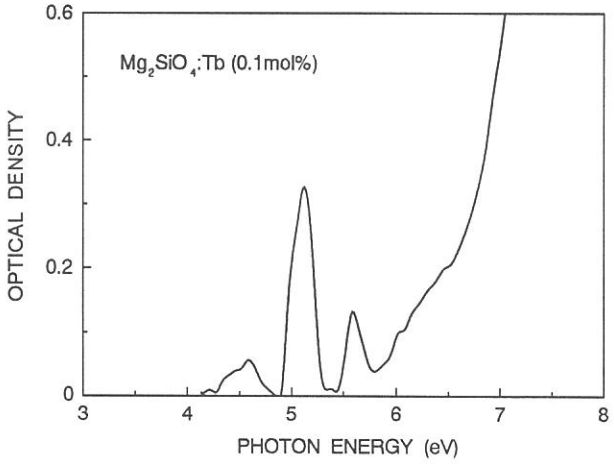

Fig. 1: Absorption spectrun of Mg_2SiO_4:Tb (0.1mol%) at 10 K.

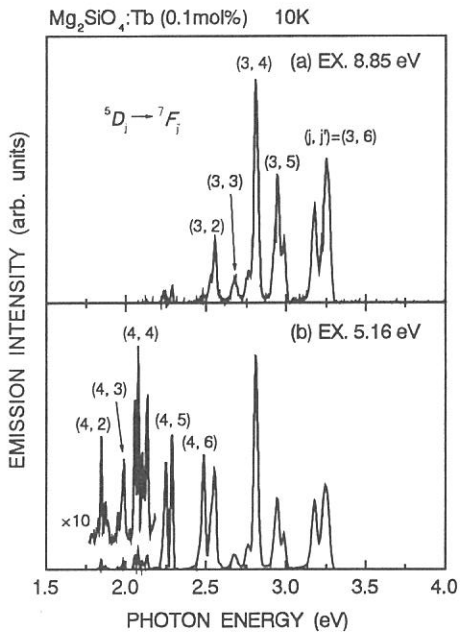

Fig. 2: Emission spectra of Mg_2SiO_4:Tb (0.01 mol%) at 10 K under excitation in (a) the fundamental region and in (b) the $4f \rightarrow 5d$ absorption region.

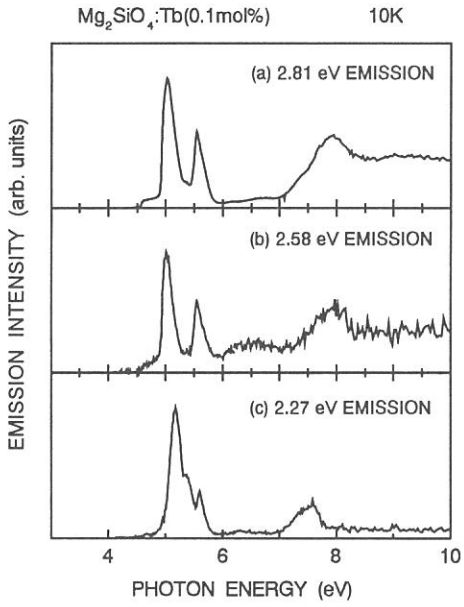

Fig. 3: Excitation spectra for the emission bands at (a) 2.81, (b) 2.58 and (c) 2.27 eV at 10 K.

[2], it is most likely that the emission bands in Figs. 2 (a) and (b) result from the $^5D_j \rightarrow {}^7F_j$ transitions in the Tb^{3+} ion.

Excitation spectra for the emission bands at (a) 2.81, (b) 2.58 and (c) 2.27 eV emission bands are shown in Fig. 3. The 2.81 and 2.58 eV bands originating from the $^5D_3$ level are excited not only in the $4f \rightarrow 5d$ absorption bands, but also in the fundamental absorption region. In Fig. 2 (a), we cannot see any other emission band under excitation in the fundamental absorption region. These results suggest that energy transfer from excited states of host Mg_2SiO_4 to the $^5D_3$ level of the Tb^{3+} ions takes place efficiently. On the other hand, the 2.27 eV band originating from the $^5D_4$ level is also excited in the $4f \rightarrow 5d$ absorption region, though in this region, the excitation spectrum for the 2.27 eV band is different from those for the 2.81 and 2.58 eV bands. Furthermore, it is scarcely excited in the fundamental absorption region. That is, the 2.27 eV band is not produced by energy transfer from host Mg_2SiO_4. The reasons for the differences in the excitation features of the 2.27 eV band from the 2.81 and 2.58 eV bands are not clear.

References

[1] D.Meiss, W.Wischert and S.Kemmler-Sack: Phys. Stat. Sol. (a) **141** (1994) 495.

[2] P.A.Arsenev, K.E.Bienert and A.V.Potemkin: Phys. Stat. Sol. (a), **26** (1974) K71.

(BL-1B)

Multi Lanthanide Doped Fluoride Phosphors for VUV Excitation

T. Kunimoto, R. Yoshimatsu, K. Ohmi and S. Tanaka

Dept. of Electrical and Electronic Eng., Tottori University
Koyama, 4-101, Tottori, Japan, 680-8552

There has been a growing interest recently in the luminescent spectroscopy of lanthanide ions in the vacuum ultraviolet (VUV) region. This has become important because of the need for new phosphors with high quantum efficiencies under VUV excitation and high stability in the plasma environment for VUV applications such as mercury free lamps and plasma display panels (PDPs). Three aspects are important in the development of VUV phosphors : a higher efficiency, a higher stability, and an optimum VUV absorption. For VUV applications, Xe discharge such as 147 nm resonance line and 173 nm excimer band are used as excitation radiation sources. However the power efficiency is quite low because of large stokes shift resulting from the conversion of one VUV photon (> 8 eV) to only one visible photon (1.6~3.2 eV), and the energy transfer probability is relatively small due to the enormously large absorption coefficient in the fundamental absorption of oxide host. To overcome this problem, a concept based on a combination of two or more lanthanide ions which is termed as quantum cutting through down conversion in large band gap material has been reported.[1-3] Other possibility for obtaining higher efficiency VUV phosphors is employing a sensitizer together with the emitting ions or activators in the fluoride host which is transparent in VUV region. The sentitizer efficiently absorbs the VUV radiation and transfers this energy efficiently to the activators. As a possible sentitizer for VUV region we investigated Pr^{3+} ion in fluoride host such as YF_3. The lowest $4f5d$ band of Pr^{3+} ion in YF_3 is predicted to lie above 45000 cm^{-1}[4]. If another lanthanide ion whose $4f$ energy levels happen to coincide with this $4f5d$ band of Pr^{3+} is incorporated in fluoride host, it might be possible for Pr^{3+} ion after absorbing VUV excitation photon to transfer this energy to the $4f$ levels of the incorporated ion instead of relaxing to its $^1S_0$ energy level which lies just below the $4f5d$ band. In this paper, we report our preliminary studies of YF_3:Pr, Gd phosphors under VUV excitation. The enhancement of Gd^{3+} 311 nm emission line with addition of Pr^{3+} ions and the quantum cutting phenomena in Gd^{3+} were observed.

Gd and Pr co-doped YF_3 phosphors were prepared by conventional solid state reaction. Powder samples were first fired at 200 °C for 1 hour and subsequently fired at 1000 °C for 3 hours in Ar atmosphere. Photoluminescence (PL) and PL excitation spectra of the phosphors were measured by BL-1B line of UVSOR. The PL spectra for $Y_{0.7-y}Gd_{0.3}Pr_yF_3$ under 170 nm excitation are represented in Fig. 1. In the range from 300 to 600 nm (16670 ~ 33330 cm^{-1}), the strong emission line of Gd^{3+} at 311 nm (32100 cm^{-1}) and a very weak emission at 407 nm (24570 cm^{-1}) of Pr^{3+} are observed. Above 300 nm (> 33330 cm^{-1}), the weak emission lines due to the ^6D_J - $^8S_{7/2}$ and ^6I_J - $^8S_{7/2}$ were observed. In addition the weak emission line was observed at about 611 nm (16370 cm^{-1}), which shhould correspond to ^6G_J - ^6P_J transitions. We consider that the observation of these emission lines is one of the confirmation of quantum cutting phenonena in Gd^{3+} ion. The peak intensity of Gd^{3+} 311 nm emission increases with increasing Pr content reaching a maximum at y=0.1. It can be seen that the Gd^{3+} 311 nm emission increased by about 5 times in comparison to y=0 sample. To clarify this enhancement, PL excitation spectra of the Gd^{3+} 311 nm emission for both $Y_{0.7}Gd_{0.3}F_3$ and $Y_{0.6}Gd_{0.3}Pr_{0.1}F_3$ were measured. As shown in Fig. 2, with the addition of Pr, a large increase in the excitation band which is mainly for corresponding state above ^6G_J levels of Gd^{3+} is found. The increased excitation band is based on the $4f5d$ absorption band of Pr^{3+}. A possible enhancement mechanism can be represented as follows. The VUV excitation energy is absorbed by $4f5d$ band of Pr^{3+} and the excited electron relaxes to the bottom of $4f5d$ band which is estimated to lie at about 48000 cm^{-1}. In $Y_{0.99}Ce_{0.01}F_3$, we have observed $4f$-$5d$ emission band

with the Stoke's shift of about 5000 cm^{-1}. In $Y_{1-z}Pr_zF_3$, we have observed only $4f^2$-$4f^2$ emissions, and this phenomenon can be explained by configuration coordinate model using the speculation that the Stoke's shift of the lowest $4f5d$ -$4f^2$ emission of Pr^{3+} is about 6000 cm^{-1}. The lattice constant of $Y_{0.6}Gd_{0.3}Pr_{0.1}F_3$ is larger than YF_3. In $Y_{0.6}Gd_{0.3}Pr_{0.1}F_3$, we therefore speculate the energy of $4f5d$-$4f^2$ emission of Pr^{3+} to be about 49000 cm^{-1} (Stoke's shift ; ~3000 cm^{-1}). In $Y_{0.6}Gd_{0.3}Pr_{0.1}F_3$, instead of $4f5d$-$4f^2$ emission of Pr^{3+}, this energy is immediately transferred to the ^6G_J and above levels of Gd^{3+} by resonant energy transfer. This excited state relaxes to the lower ^6D_J, ^6I_J and ^6P_J through the nonradiative processes ($^6G \rightarrow {}^6D \rightarrow {}^6I \rightarrow {}^6P$) and the radiative process ($^6G \rightarrow {}^6P$), resulting in the enhanced Gd^{3+} 311 nm emission corresponding to ^6P_J-$^8S_{7/2}$ transition.

In conclusion the enhancement of Gd^{3+} 311 nm emission (^6P_J-$^8S_{7/2}$) in YF_3 host with the addition of Pr was observed. The energy transfer from this level to other $4f$ levels in suitable activators such as Eu and Tb may produce efficient VUV phosphors.

This work is supported by "Research for the Future Program" through grant JSPS-RFTF 96 R12501 from Japan Society for the Promotion of Science (JSPS)".

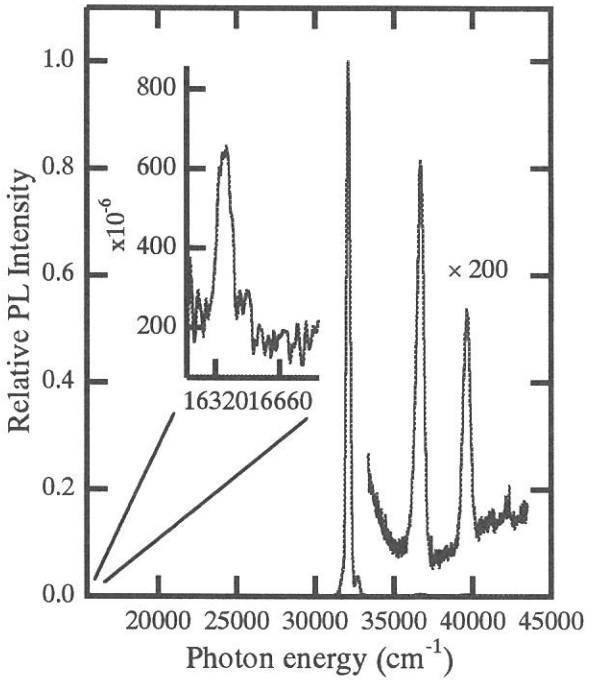

Fig. 1 PL spectra of $Y_{0.6}Gd_{0.3}Pr_{0.1}F_3$ for 170 nm excitation. The inset shows the magnification of emission spectrum around 16500 cm^{-1}. The intensity is normlized by the peak height of Gd^{3+} 311 nm (32100 cm^{-1}) emission.

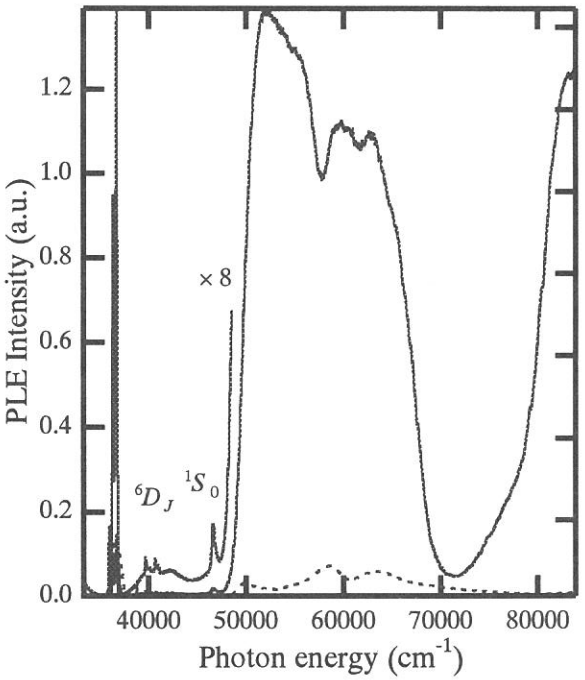

Fig. 2 PL excitation spectra of $Y_{0.6}Gd_{0.3}Pr_{0.1}F_3$ (solid line) and $Y_{0.7}Gd_{0.3}F_3$ (broken line) monitored at 311 nm emission line of Gd^{3+} ion. ^6D_J and ^6I_J levels of Gd^{3+} and $^1S_0$ level of Pr^{3+} can be observed.

REFERENCE

[1] R. T. Wegh, H. Donker, A. Meijerink, R. J. Lamminmäki and J. Hölsä: Phys. Rev. **B56**(1997)13841.

[2] R. T. Wegh, H. Donker, K. D. Oskam and A. Meijerink: Science **283**(1999)663.

[3] R. T. Wegh, E. V. D. van Loef and A. Meijerlink: J. Lumin. **90**(2000)111

[4] W. W. Piper, J. A. DeLuca and F. S. Ham: J. Lumin. **8**(1974)344.

(BL-1B)

Reflection Spectra of Ethyl-Ammonium Cadmium Halides and Ethyl-Ammonium Halides

Akimasa OHNISHI[A], Takafumi OTOMO[A] and Mamoru Kitaura[B]

[A]*Department of Physics, Yamagata University, Yamagata 990-8560*

[B]*Fukui National College of Technology, Sabae 916-8507*

So far, we have investigated optical reflection spectra of $(C_2H_5NH_3)_2CdCl_4$ layered crystals to clarify the energy band structure.[1,2] In this materal, two types of exciton absorption bands are observed at 6.2 and 8.2 eV at 7 K. We proviously assigned that the 6.2 eV band comes from the electronic transition from the Cl^- $3p$ VB to the Cd^{2+} $5s$ CB, and the 8.2 eV band that from the Cl^- $3p$ VB to the NH_3^+ s-like CB. As for the assignment of the 8.2 eV band, however, there still remains ambiguity. In the present study, the reflection spectrum of $C_2H_5NH_3Cl$ layered crystal has been investigated to obtain the information about the origin of the 8.2 eV exciton band in $(C_2H_5NH_3)_2CdCl_4$. The reflection spectra for $(C_2H_5NH_3)_2CdBr_4$ and $C_2H_5NH_3Br$ layered crystals have been also investigated.

$(C_2H_5NH_3)_2CdBr_4$ crystals were grown by slow evaporation method from the aqueous solution of stoichiometric amount $C_2H_5NH_3Br$ and $CdBr_2$ at room temperature in dark. $C_2H_5NH_3Cl$ and $C_2H_5NH_3Br$ crystals were also obtained by the similar method. Experiments were perforemed at the BL-1B of UVSOR equipped with a 1m Seya-Namioka VUV monochromator. Reflection spectra from samples for the polarization perpendicular to the c-axis (E⊥c) were measured with a combination of a photomultiplier (Hamamatsu R105) and sodium salycilate phosphor.

Figures 1(a) and (b) show the reflection spectra of the cleaved surface of $(C_2H_5NH_3)_2CdCl_4$ and $C_2H_5NH_3Cl$ at 7 K in the range of 3-30 eV for E⊥c. The reflection spectrum of $(C_2H_5NH_3)_2CdCl_4$ is the same as that reported in previous paper.[2] In $C_2H_5NH_3Cl$, the lowest exciton absorption band is observed at 7.8 eV, which is located at the energy position similar to the 8.2 eV band in $(C_2H_5NH_3)_2CdCl_4$. The band-peak energy is in good agreement with that of the lowest exciton band in NH_4Cl.[3] This agreement indicates that the VB and the CB of $C_2H_5NH_3Cl$ are constructed from the Cl^- $3p$ and the NH_3^+ s-like states, respectively. Thus, it is most likely that the 8.2 eV band of $(C_2H_5NH_3)_2CdCl_4$ comes from the electronic transition from the Cl^- $3p$ VB to the NH_3^+ s-like CB, being in line with our previous assignment.

Figure 2(a) shows the reflection spectrum of $(C_2H_5NH_3)_2CdBr_4$ at 10 K for E⊥c in 3-20 eV. Two exciton bands with splitting energy of 0.5 eV are observed at 4.9 and 5.4 eV. Since the splitting energy is comparable with the spin-orbit splitting energy of a Br atom, they are related to the transition from the VB constructed from Br^- $4p$ states (so-called halogen doublet). In addition, the band-peak energies agree well with those of the lowest exciton bands in $CdBr_2$.[4] Therefore, the 4.9 and 5.4 eV bands in $(C_2H_5NH_3)_2CdBr_4$ are attributed to the transitions from the Br^- $4p$ VB to the Cd^{2+} $5s$ CB. Two exciton bands with the splitting of 0.5 eV are also observed at 6.9 and 7.4 eV. By the analogy with the case of

$(C_2H_5NH_3)_2CdCl_4$, they are suggested to be due to the transition from the Br^- $4p$ VB to the NH_3^+ s-like CB.

In Fig. 2(b) is shown the reflection spectrum of $C_2H_5NH_3Br$ at 10 Kfor E⊥c in 3-20 eV. At 6.5 and 7.0 eV the peaks due to halogen doublet are observed. The peak energies of the 6.5 and 7.0 eV bands are in good agreement with those of the lowest exciton bands in NH_4Br, [3] and thus the exciton bands are attributed to the electronic transitions from the Br^- $4p$ VB to the NH_3^+ s-like CB. From this, the 6.9 and 7.4 eV bands of $(C_2H_5NH_3)_2CdBr_4$, which are peaked at the almost same energy positions as the 6.5 and 7.0 eV bands in $C_2H_5NH_3Br$, must come from the transition from the Br^- $4p$ VB to the NH_3^+ s-like CB.

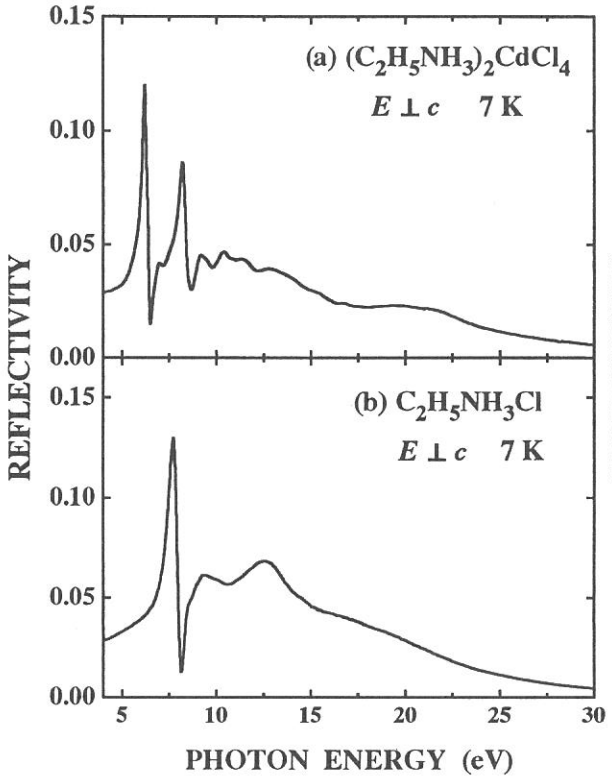

Fig.1 Reflection spectra of (a) $(C_2H_5NH_3)_2CdCl_4$ and (b) $C_2H_5NH_3Cl$ layered crystals

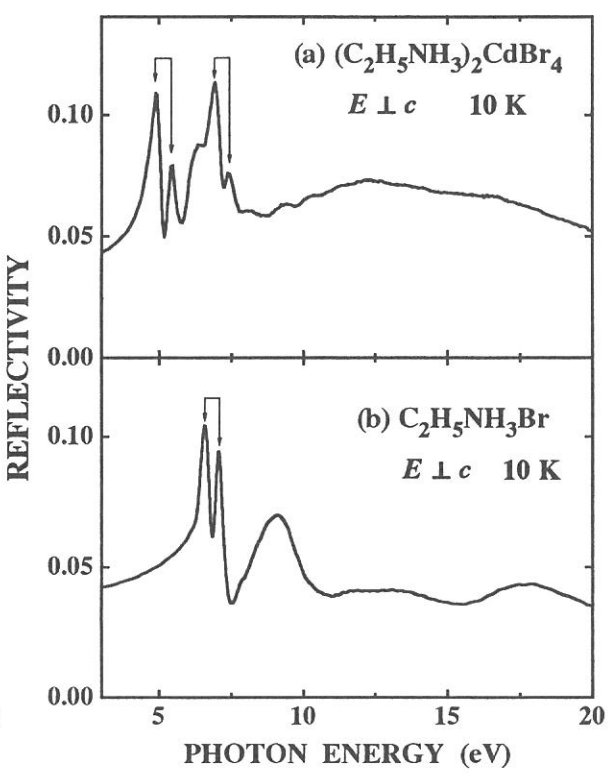

Fig.2 Reflection spectra of (a) $(C_2H_5NH_3)_2CdBr_4$ and (b) $C_2H_5NH_3Br$ layered crystals

References

1) A. Ohnishi, K. Tanaka and T. Yoshinari: J. Phys. Soc. Jpn. **68** (1999) 288.

2) A. Ohnishi, K. Tanaka, T. Otomo, T. Yoshinari and M. Kitaura: UVSOR-27, *p.*80.

3) H. Yamashita: J. Phys. Soc. Jpn. **29** (1990) 338.

4) M. Fujita, H. Nakagawa, H. Matsumoto, T. Miyanaga, M. Watanabe, K. Fukui, E. Ishiguro, Y. Fujii and Y. Sakisaka: J. Phys. Soc. Jpn. **59** (1990) 338.

(BL1B)

Fluorescence Spectra of Uniaxially Oriented Polyethylene 2,6-Naphthalate Films

Isuke OUCHI, Ikuo NAKAI[A] and Masao KAMADA[B]

Faculty of Engineering, Tokushima Bunri University, Shido, Kagawa 769-2193
[A]Faculty of Engineering, Tottori University, Koyama, Tottori 680-8552
[B]UVSOR, Institute for Molecular Science, Myodaiji, Okazaki 444-8585

Polyethylene 2,6-naphthalate (PEN) is a polyester having naphthalene rings in the main chain, one each in a repeat unit. The fluorescent nature of PEN has been known since long ago. The first description about it appeared in 1969;[1] high-energy electron excited luminescence of PEN films was compared with that from dimethyl 2,6-naphthtalate solutions and crystals, indicating that the former was broader and shifted its peaks toward longer wavelengths. The red shift therein was interpreted to be due to emission from excimer states. Since then, several researchers including one of the present authors treated the luminescence of PEN for various purposes.[2-4] According to them, the excitation peaks nearly corresponded to those of absorption; and the fluorescence spectrum looked roughly like a mirror image of the absorption. Its fluorescence occurred from the lowest energy level of the singlet excited states, which was conformed to the Kasha law.

In the present study, it was intended to look into the emission behaviour of PEN in the vacuum ultraviolet region and also to reveal more details of the spectrum in the ultraviolet and visible regions in respect to the molecular orientaion.

Relatively thick samples of undrawn, uniaxially or biaxially drawn films of 60-100 μ m thickness, were supplied from the Film Research Laboratory of Teijin Limited. Cut samples of 10 - 15 mm square were held by screws between a copper frame and a holder, keeping the original machine direction. Eight circular holes of 10 mm diameter were opened in the copper holder plate; eight samples were measured during a series of experiments.

The Seya-Namioka type monochromator installed at the BL-1B was utilized for reflection and emission measurements in the range between 500A and 6500A. In most cases, the G3 grating of 600 lines/mm was utilized. Incidence angle was set as 12.5° for reflection measurements. The exit slit width was set as 100 μ m for reflection and overall excitation measurements; here, the overall excitation spectra mean the spectra taken without filter nor monochromator for emitted light. Namely, only excitation light is monochromatized by a grating; and the observed light intensity is the sum of all the light of various wavelenghts emitted from the sample and passed through the detector window. Therefore, one concerns only which wavelength of incident light is effective to excite the luminescence. Contribution of stray light to the luminescence was corrected by substracting the fluorescence taken with a pyrex glass before the sample; this correction was less than 1 %. In the measurements of fluorescence or ordinary excitation spectra, the slit width was set as 500 μ m; fluorescence was lead to the MIC monochromator placed outside of the vacuum chamber. Although the incident light is fairly polarized as a nature of synchrotron radiation, the emitted light was detected without polarizers.

Separate measurements were further made by use of Shimazu Fluorescence Spectrometer Model RF 5300PC with a xenon lamp as light source. A pair of polarizers were placed before and after the sample, when necessary. A Jusco spectrometer, consisting of a monochromator for excitation and a double monochromator for luminescence, having a halogen lamp as a source was also used in parallel.

An example of the overall excitation spectra is shown in Fig. 1, for a biaxialy drawn PEN film, where

absorption spectra of a uniaxially drawn PEN film[5] are superposed on the overall excitation spectra. If looked at closer, the excitation peaks therein correspond to the tails of the absorption rather than the peaks. This may be related to the fact that the intensity of fluorescence increases with the depth reached by the incident light, depending on the absorption coefficient at the wavelength of emitted light.

Although effects of stray light were corrected, there may be some effects of reflected light by scattering. Nevertheless, it seems that there must be a considerable amount of emission in vacuum ultraviolet region on top of the detected fluorescene in ultraviolet region.; because, the excitation at 1200A gave rise to only about tenth of the fluorescence if observed at 4300A, comparing with those excited at 2500A and observed at 4300A. This problem is yet to be examined.

Fig. 2 shows the fluorescence spectra of undrawn PEN films taken with a pair of polarizers before and after the specimen; this measurement was made separately by use of Shimazu Fluorescence Spectromer RF5300PC. Since undrawn films are isotropic in the film plane, these curves indicate that the monochromator for emission is horizontally polarized in this wavelength region. (Monochromator for incidence light has the same character.) Furthermore, Fig. 2 indicates that the fluorescence of PEN is composed of two peaks about 200A apart; also, the longer wavelength peak at about 4550A is parallel-polarized, as clearly manifested by measurements by use of uniaxially drawn films, which are not shown here.

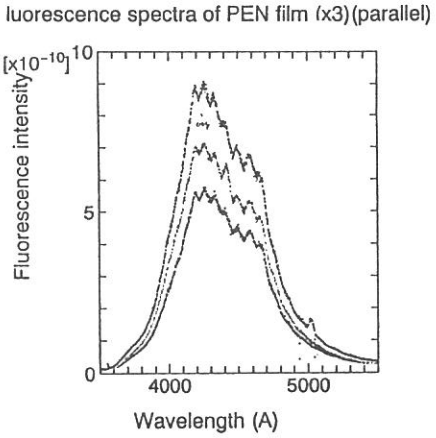

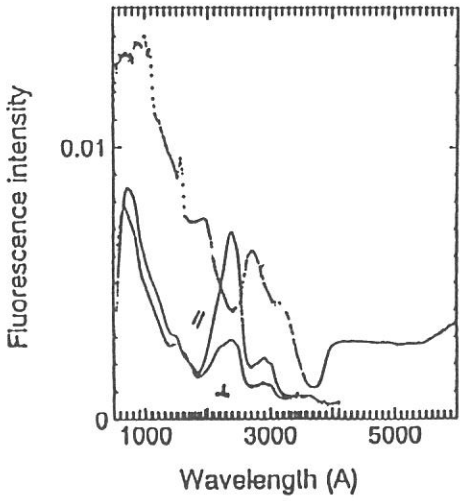

Fig. 1. Overall excitation spectra of a biaxially drawn PEN film (Upper curve). Lower curves are the absorption spectra, either parallel or perpendicular, of a uniaxially drawn PEN film in an arbitrary unit.

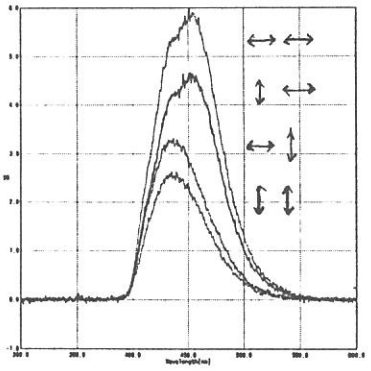

Fig. 2. Fluorescence of undrawn PEN films excited at 3500 A. First arrow indicates the polarization of incident light, and the second that of fluorescence.

Fig. 3 shows an example of fluorescence spectra of a uniaxially drawn PEN film excited at 2550A, 2000A, 3500A (from the top to the bottom), where the electric vector of the synchrotron radiation was parallel to the draw direction. In addition to the two components shown in Fig. 2, fine structures are clearly manifested. Further analyses are yet to be made.

1. D.H. Phillips and J.C. Schug, J. Chem. Phys., 50 (1969) 3297.
2. I. Ouchi, M. Hosoi and F. Matsumoto, J. Appl. Polym. Sci., 20 (1976) 1983.
3. P.-S. Cheung, C.W. Roberts and K. Wagener, ibid 24 (1979) 1809.
4. I. Ouchi, R. Miyamura, M. Sakaguchi, S. Hosaka and M. Kitagawa, Polym. Adv. Technol., 10(1999)195.
5. I. Ouchi, I. Nakai and M. Kamada, UVSOR Act. Rept. 1999,(2000) 82.

(BL1B)

Photoluminescence in Polypropylene Induced by Ultraviolet Laser Irradiation

Takehiko TOYODA, Hiromitsu KATO, Toshihide ITO, Naoshi HIRAI and Yoshimichi OHKI
Department of Electrical, Electronics, and Computer Engineering, Waseda University
Shinjuku-ku, Tokyo 169-8555

Category 4. Solid- and liquid- phase spectroscopy 1 (IR, VUV, etc)

I. EXPERIMENTAL PROCEDURES

The samples tested are PP sheets of 50 μm thick. The sample is just general PP sheets, in which some kinds of additives and antioxidants are added. This material only contains saturated C-C and C-H bonds which are not chromophores. Therefore, in PP, luminescence contribution of chromophores is rather low leading to an easier observation of luminescence due to degradation. We have measured photoluminescence (PL) spectra and photoluminescence excitation (PLE) spectra induced in PP by irradiation of photons from an ArF excimer laser (photon energy: 6.4 eV, power intensity: ca 50 mJ/pulse, repetition frequency: 1 Hz) and synchrotron radiation (SR) at BL1B line in UVSOR at 300 K.

II. RESULTS AND DISCUSSION

The PL spectrum excited by synchrotron radiation photons with an energy of 6.4 eV at 300 K is shown in Fig. 1. The change of the PL spectrum as a function of the irradiation time is shown in Fig. 2 for the case that the excitation by the ArF excimer laser was continued in air at room temperature. Because the repetition frequency of the laser was 1 Hz, it is thought that the temperature increase and its effect on the chemical change are negligible. The luminescence around 4 eV decreases rapidly with continuous laser irradiation, and a new luminescence band with a peak around 3 eV is induced. The luminescence due to the oxidation that relates essentially to the degradation of PP is examined by comparing luminescence spectrum induced by the irradiation in a vacuum and the one induced in an O_2 atmosphere. So, the PL spectra are compared in Fig. 3 between two cases where the sample was put in vacuum (1×10^{-1} Pa) and in oxygen at 1 atm at room temperature. The PL intensity is found to be enhanced significantly around 3 eV by the irradiation in vacuum, although it diminishes almost completely if irradiated in oxygen.

As an alternative possibility, it is considered that the excitation band has been moved to an energy different from the one of the ArF excimer laser (= 6.4 eV). Therefore, the PLE spectrum was measured using synchrotron radiation at 300 K in a vacuum at 1.3×10^{-7} Pa for the samples that had been irradiated by the ArF excimer laser for 1000 s either in air, in oxygen, or in vacuum at room temperature. The PLE spectra obtained at different detecting energies (4.1, 3.5, and 2.9 eV) are shown in Fig. 4. The PL intensity becomes smaller with an increase in the oxygen content of the atmosphere. In Fig. 4(a), it is also found that the PLE spectrum measured after the irradiation in vacuum has its peak at a lower energy than the peak position before irradiation.

As for the PLE spectra detected at 3.5 eV, the intensity becomes larger and a new PLE band appears around 5.7 eV if the sample was irradiated in vacuum, while the PL intensity becomes smaller for the samples irradiated in air or in oxygen. When the PLE was detected at 2.9 eV, the PL was observable only in the sample that had been irradiated in vacuum as shown in Fig. 4(c). These results suggest that different chemical groups were formed through different processes depending on the point that oxygen was present or not when the sample was irradiated for 1000 s by the ArF excimer laser. Namely, the luminescence center disappears by the continuous photon irradiation in the presence of oxygen, while a new luminescence center is induced by similar irradiation if oxygen is not present.

When the photons from an ArF excimer laser are irradiated to PP, the luminescence component around 4 eV decreases with an increase in irradiation time irrespective of the irradiation atmosphere. This is probably due to the decomposition of unsaturated ketone which is present in PP as an impurity. The luminescence component

around 3 eV increases with an increase in irradiation time only in the case that the laser irradiation was done in vacuum. This is probably caused by the double bonds induced by the irradiation. These results suggest that different chemical groups are induced depending on the irradiation atmosphere.

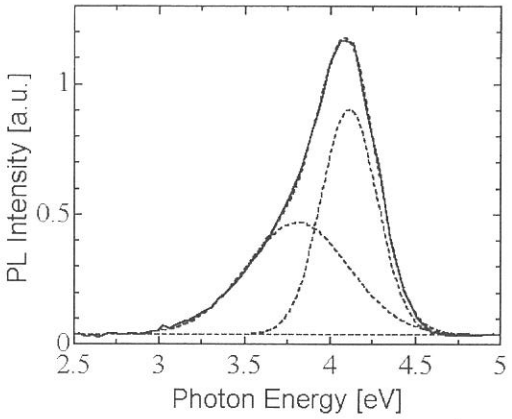

Fig.1. PL spectrum excited at 6.4 eV induced in PP by irradiation of photons from synchrotron radiation, and its Gaussian-fit spectra.

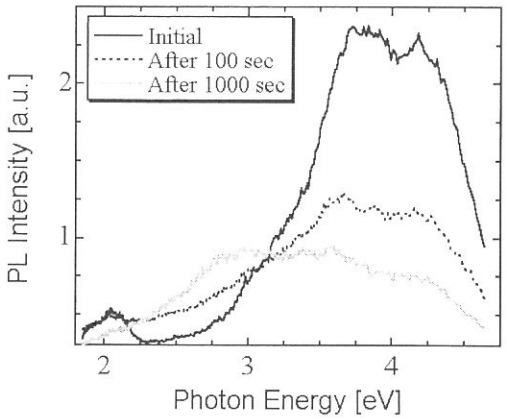

Fig.2. Change of PL spectrum excited by the excimer laser photons with irradiation time in air at room temperature.

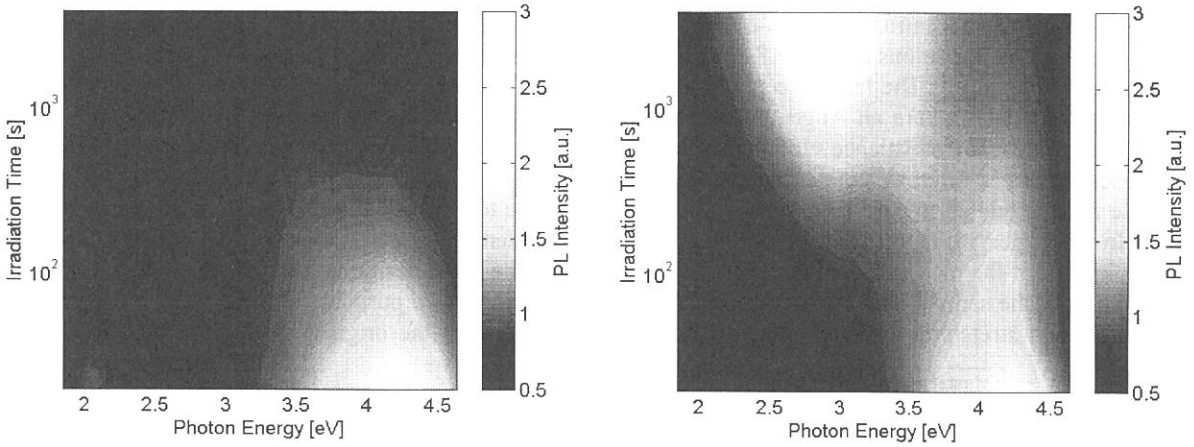

Fig.3. Change of PL spectrum with irradiation time excited by the excimer laser photons in oxygen (a) or in vacuum (b) at room temperature.

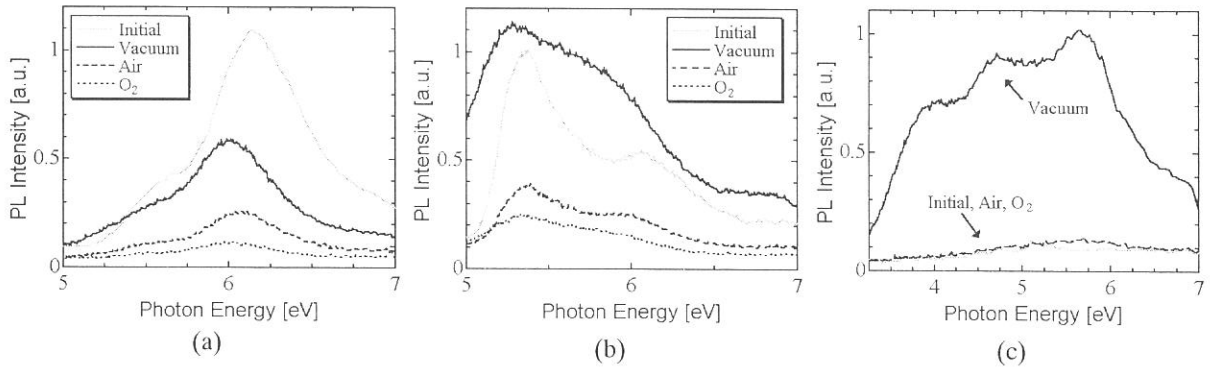

Fig.4. PLE spectra measured using synchrotron radiation.
Detected at 4.1 eV (a), at 3.5 eV (b), and at 2.9 eV (c).

(BL1B)

Laser-Induced Increase of Auger-free Luminescence under Excitation of Core-Electrons in BaF_2

T. Tsujibayashi[a], J. Azuma[b], K. Hayakawa[c], M. Horimoto[c], M. Itoh[c], M. Watanabe[d], O. Arimoto[e], S. Nakanishi[f], H. Itoh[f], S. Asaka[g*], and M. Kamada[h]

[a]*Department of Physics, Osaka Dental University, Hirakata 573-1121*
[b]*Department of Physics, Kyoto University, Kyoto 606-8502*
[c]*Department of Electrical & Electronic Engineering, Shinshu University, Nagano 380-8553*
[d]*Department of Fundamental Sciences, Kyoto University, Kyoto 606-8501*
[e]*Department of Physics, Okayama University, Okayama 700-8530*
[f]*Department of Advanced Materials Science, Kagawa University, Takamatsu 760-8526*
[g]*Equipment Development Center, Institute for Molecular Science, Okazaki 444-8585*
[h]*UVSOR Facility, Institute for Molecular Science, Okazaki 444-8585*

We have been developing a spectroscopic system in which both synchrotron radiation (SR) and laser are used [1, 2]. The system is designed for investigation of dynamical behaviors of excitations in inner-shell electronic states of solids through non-linear spectroscopy such as two-photon and pump-probe spectroscopy. The wide spectral range of SR, from X-ray to infrared, and the high power of lasers are combined in the system.

BaF_2 is known as a scintillator with 6-eV luminescence in high-energy physics. The luminescence is observed under excitation with photons above 17.8 eV. This energy corresponds to that between the outermost core state to the conduction band [3]. The luminescence is attributed to the transition of a valence electron to the hole in the outermost core state, where an Auger process is suppressed since the energy released by the transition is not enough to excite another valence electron to the conduction band. The luminescence is known as Auger-free luminescence (AFL) or cross luminescence.

Since AFL is related to core holes, it should be a good probe to examine the relaxation of core electrons and holes. In this paper, we report laser-induced increase of AFL intensity of BaF_2 under excitation through SR. The block diagram of the measuring system is depicted in Fig. 1. The basic design is the same as that in Ref. 2. The temperature of the sample was 295 K. An optical fiber was used for two purposes: introducing the laser light to the sample and stretching the laser pulse to 0.5 ns. The duration of the original laser pulse was 160 fs. The

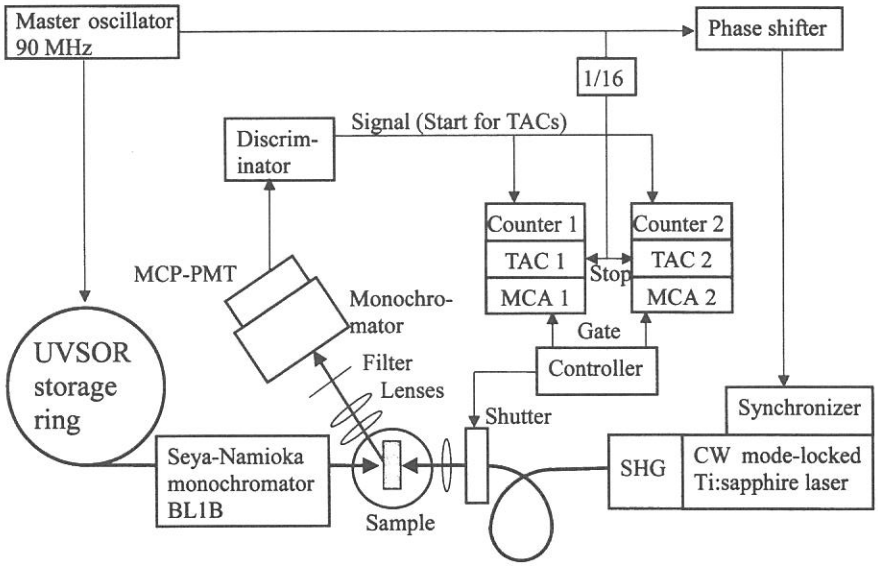

Fig. 1 The block diagram of the experimental setup.

---

*Present address: *Elementary and Secondary Education Bureau, Ministry of Education, Culture, Sports, Science and Technology, Tokyo 100-0013.*

shapes of excitation pulses of the laser and SR are shown in panels (a) and (b), respectively, of Fig. 2.

Panels (c) and (d) of Fig. 2 show the time responses of the AFL under the simultaneous excitation by SR and laser and the excitation by SR alone, respectively. The photon energy of SR was 18.4 eV. The signal was accumulated for about an hour for each curve. The humps at –12.5 ns are not caused by AFL or other luminescence [4]. The absence of signal at 11 ns indicates that the filter and monochromator prevent the false light-signal due to the scattered laser-light completely.

The intensity of AFL under SR-laser excitation is larger by several percent than that under excitation by SR alone as shown in Fig. 2. However, the ratio of the increase was varied significantly in separate measurements at the same beam line.

Searching for the cause of this uncertain value of the ratio, we noticed the existence of defects in the sample at low temperatures. Defects-related enhancement of luminescence under SR-laser excitation was reported previously [5]. In this report, a crystal of BaF_2 was kept 15 K and luminescence of self-trapped excitons was detected. We observed that the AFL intensity decreased after irradiation of SR light for a few tens hours at 295 K. It is implied that defects are created and remain to decrease the AFL intensity even at a room temperature.

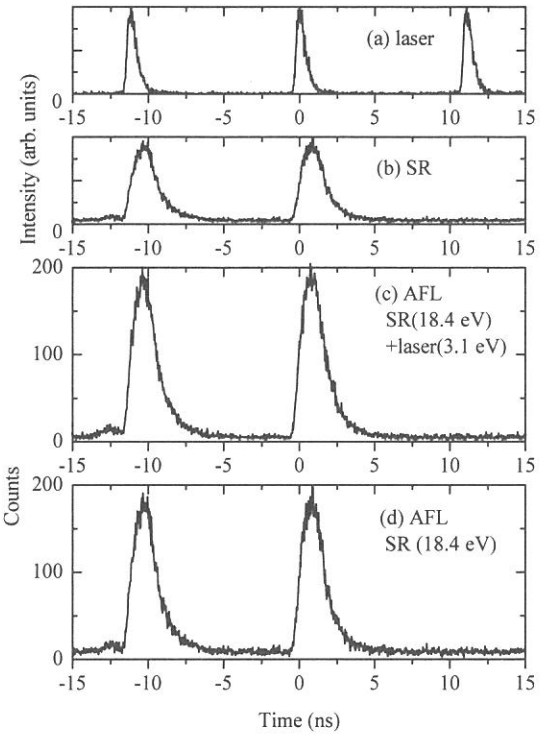

Fig. 2 Temporal behaviors of (a) laser pulses, (b) SR pulses, (c) AFL under SR-laser excitation, and (d) AFL under SR alone excitation.

If breaking defects by the laser light causes the increase of the AFL intensity, the ratio depends on the number of defects. Assuming that this number varies with the time-length of irradiation of SR prior to the measurement, there is a possibility that the increase rate varies sample to sample in separate measurements.

The present work was partially supported by a Grant-in Aid for Scientific Research from the Ministry of Education, Culture, Sports, Science and Technology.

References

[1] S. Asaka *et al.*: Rev. Sci. Instrum. **69** (1998) 1931.
[2] S. Asaka *et al.*: UVSOR Activity Report **26** (1999) 34.
[3] M. Itoh *et al.*: Solid State Commun. **65** (1988) 523.
[4] J. Azuma *et al.*: Nucl. Instrum. & Methods (in press).
[5] M. Watanabe *et al.*: UVSOR Activity Report **26** (1999) 66.

(BL1B)

Luminescence due to Self-Trapped Excitons in Orthorhombic $SnBr_2$

Y. YAMASAKI and N. OHNO

Division of Electronics and Applied Physics, Graduate School of Engineering,

Osaka Electro-Communication University, Neyagawa 572-8530, Japan

Optical properties of lead halides have been studied extensively so far by several groups. Especially, luminescence studies of these materials have been carried out since they give complimentary information on the photolysis phenomena. Orthorhombic tin halides, $SnBr_2$ and $SnCl_2$, have the same crystal structure (space group *Pmnb*) and the similar electronic configurations as orthorhombic lead halides. It is interesting to know the electronic structures and exciton states in Sn halides. The investigation of the optical properties of $SnBr_2$ and $SnCl_2$ would deepen our understanding the energy relaxation processes in this system. However, only a few studies on optical properties of Sn halides have been reported so far. [1-3]

Reflection measurement of $SnBr_2$ has revealed a pronounced polarization dependence of the first exciton band at 3.4 eV.[4,5] The polarization dependence has been well interpreted as a cationic interband transition in Sn^{2+} ($5s \rightarrow 5p$) under the crystal field with C_S symmetry.[5] Moreover, the observed first exciton structures in $SnBr_2$ are considerably sharp as compared with those in orthorhombic Pb halides.[6,7] The exciton binding energy has also been estimated as 32 meV. The logarithmic plot of the absorption spectra at the absorption edge has been found to give a straight line, [5] that is, the absorption tail of $SnBr_2$ is described as the Urbach rule. The obtained small value of the steepness parameter $\sigma_0 = 0.7$ suggests that the electron-phonon interaction is in a strong case, and the free carriers are expected to be self-trapped in $SnBr_2$.

Luminescence measurements of $SnBr_2$ single crystals were carried out at BL1B in the UVSOR facility. The samples were mounted on a copper block attached to a temperature-variable cryostat of liquid helium-flow type. The light beam passed through a 1-m Seya-Namioka type monochromator was incident on the sample surface. Luminescence emitted from the illuminated surface was collected by lenses, and analyzed through a Jovin-Yvon HR320 monochromator equipped with an R955 photomultiplier.

Figure 1 shows the luminescence spectra of $SnBr_2$ measured at 12 K. The polarization of excitation light was along the *b*-axis of the crystal. The spectrum shown by solid curve was obtained under the excitation with 3.39-eV light whose energy falls in the first exciton region. Two luminescence bands are observed at 2.17 eV and 1.85 eV. The 2.17-eV band has a Gaussian lineshape and a large Stokes shift of 1.24 eV from the lowest exciton energy for *E//b* polarization. When the excitation was made with higher-energy light than the bandgap energy, on the other hand, the luminescence spectrum changed drastically as shown by hatched curve in the figure, where the excitation energy was 6.20 eV. The spectrum consists of a broad band peaking at 2.52 eV, and the weak structures around 2.3 and 2.9 eV. The intensities of these luminescence bands become weak when the sample is warmed above 50 K, and almost disappear at 100 K.

Figure 2 show the excitation spectra for the 2.17-eV band (solid) and 2.52-eV band (hatched) measured at 12 K. Arrows indicate the first exciton energies for *E//b* polarization. As clearly seen, the 2.17-eV band is efficiently produced under the photo-excitation in the first exciton region. On the other hand, the 2.52-eV luminescence is hardly excited under the exciton region, but stimulated by photons with energies higher than the bandgap. It is thus confirmed that under excitation in the lowest exciton band the

2.52-eV luminescence is not observed while the 2.17 eV luminescence appears strongly. Although not shown in the figure, the excitation spectrum for the 1.85-eV band exhibits a strong peak at 3.11 eV, suggesting this band is ascribed to some impurity.

There have been found two types of luminescence in $PbBr_2$ at low temperatures.[8,9] One is the B luminescence (2.75 eV) produced under the excitation in the first exciton region, attributed to the radiative decay of self-trapped excitons at Pb^{2+} ion sites in $PbBr_2$. The other is the BG luminescence (2.62 eV) stimulated by photons with energies above the band gap, which originates from tunneling recombination of holes released from some trapping centers with electrons trapped at the Pb_2^{3+} STEL centers.[10] The 2.17-eV band in $SnBr_2$ is probably ascribed to self-trapped excitons similar to the B band in $PbBr_2$ since the 2.17-eV band appears under the excitation of the first exciton region, that is, this band is originated from the radiative decay of self-trapped excitons at Sn^{2+} ion sites. On the other hand, it is probable that the origin of the 2.52-eV band is due to the similar relaxed excited states to the BG luminescence in $PbBr_2$, namely the tunneling recombination of holes with electrons trapped at the Sn_2^{3+} STEL centers.

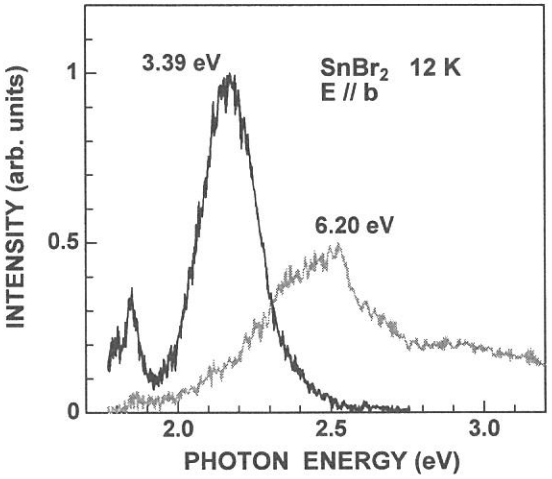

Fig. 1. Luminescence spectra of $SnBr_2$ excited with 3.39-eV light (solid) and 6.20-eV light (hatched) with *E//b* polarization at 12 K.

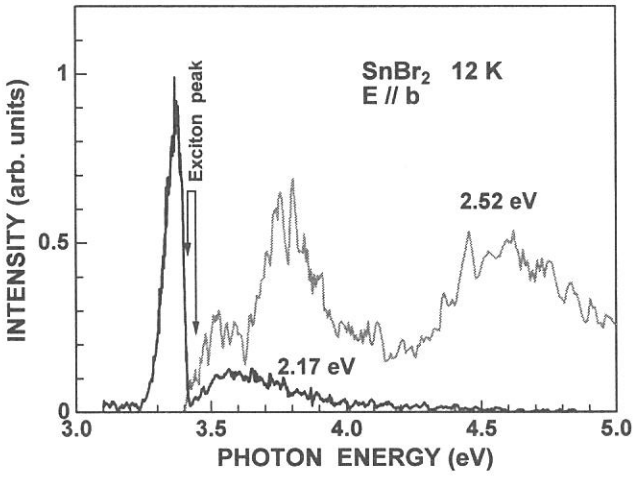

Fig. 2. Excitation spectra for 2.17-eV (solid) and 2.52-eV band (hatched) of $SnBr_2$ measured at 12 K.

References

[1] N.S. Pidsyrailo, A.S. Voloshinovskii, N.G. Stan'ko and Z.A. Khapko: Sov. Phys. Solid State **24** (1982) 708.
[2] A.S. Voloshinovskii, S.V. Myagkota, N.S. Pidsyrailo and Z.A. Khapko: Opt. Spectrosc. **52** (1982) 457.
[3] A.S. Voloshinovskii: Phys. Solid State **35** (1993) 1588.
[4] Y. Yamasaki and N. Ohno, UVSOR Activity Report **1999** (2000) 84.
[5] N. Ohno, Y. Yamasaki, H. Yoshida and M. Fujita, Phys. Status Solidi (b), in press.
[6] J. Kanbe, H. Takezoe and R. Onaka, J. Phys. Soc. Jpn. **41** (1976) 942.
[7] M. Fujita, H. Nakagawa, K. Fukui, H. Matsumoto,T. Miyanaga and M. Watanabe, J. Phys. Soc. Jpn. **60** (1991) 4393.
[8] M. Kitaura and H. Nakagawa: J. Electron Spectrosc. and Relat. Phenom. **9** (1996) 171.
[9] M. Kitaura and H. Nakagawa: J. Lumin. **72-74** (1997) 883.
[10] S.V. Nistor, E. Groovaert and D. Schoemaker: Phys. Rev. **B48** (1993)9575.

(BL1B)

Energy Transfer from Pr^{3+} to Eu^{3+} Ions through Gd^{3+} Sublattices in $NaGdF_4$:Pr,Eu

T. HIRAI[A] and N. OHNO[B]

[A]*Graduate School of Engineering Science, Osaka University, Toyonaka 560-8531, Japan*
[B]*Division of Electronics and Applied Physics, Graduate School of Engineering, Osaka Electro-Communication University, Neyagawa 572-8530, Japan*

Recently, the phosphors to convert vacuum ultraviolet (VUV) photons into visible photons, which are used in mercury-free fluorescent lamps and plasma display panels, have been researched extensively. The materials with a higher quantum efficiency and higher stability for VUV light emitted from Xe dimers (172 nm) and/or monomers (147 nm) are naturally quite needed.

In some of rare-earth activated fluorides, the conversion of one VUV photon into two visible photons is reported to be possible. Such a phenomenon is called "quantum cutting" or "quantum splitting". This indicates that these VUV phosphors have quantum efficiency more than 100%. Especially, $LiGdF_4$:Eu phosphor has been reported to convert one VUV photon into two visible (red) photons with a quantum efficiency close to 200% [1]. This conversion is caused by the energy transfer from the Gd^{3+} site, which absorbs one VUV photon, to two Eu^{3+} ions which emit two red-light photons. However, the *f-f* transition in the Gd^{3+} site is dipole-forbidden in origin, so that the absorption of the VUV photons is quite weak. On the other hand, it has been reported in $NaGdF_4$:Ce,Eu that the absorbed UV-photon energy in Ce^{3+} ions due to the allowed *f-d* transition transfers to Eu^{3+} ions through Gd^{3+} sublattices [2]. In the same manner, Pr^{3+} ions are expected to act as a suitable sensitizer to the VUV photons emitted from a high-pressure Xe discharge at around 172 nm, since the allowed *f-d* absorption in Pr^{3+} ions in fluoride phosphors are observed at around 180 nm. In the present study, we have examined whether the energy transfer occurs or not from Pr^{3+} ions to Eu^{3+} ions in $NaGdF_4$:Pr,Eu phosphor.

On the right-hand side of Figure 1 are shown the luminescence spectra of $NaGdF_4$:Pr,Eu, $NaGdF_4$:Eu, $NaGdF_4$:Pr and $NaYF_4$:Pr at room temperature. The excitation was made by an ArF excimer laser (193 nm). Measurements of the excitation spectra for these luminescence lines are carried out with use of SOR at BL1B in the UVSOR facility. The results are shown on the left-hand side of the figure.

In $NaGdF_4$:Pr, only a luminescence line is observed at 310 nm. This luminescence line is attributed to the *f-f* transition from ^6P_J state to $^8S_{7/2}$ ground state in Gd^{3+} sublattice. It is found that the luminescence is efficiently excited at around 180 nm, which is due to the *f-d* transition in Pr^{3+} ions, since no structure is observable in the excitation spectra for phosphors without Pr^{3+} ions. This fact indicates that the energy transfer occurs from Pr^{3+} ions to Gd^{3+} sublattices in $NaGdF_4$:Pr. In $NaYF_4$:Pr, on the other hand, the *f-d* excited states in Pr^{3+} ions at around 180 nm relax immediately to $^1S_0$ state, and then emit 407-nm photons ascribed to the *f-f* transition in Pr^{3+} ions [3].

The similar energy transfer is found also to occur in $NaGdF_4$:Pr,Eu. In both $NaGdF_4$:Eu and $NaGdF_4$:Pr,Eu, all prominent luminescence lines arise from the *f-f* transition of Eu^{3+} ions. The luminescence line at 615 nm is attributed to the transition from $^5D_0$ to $^7F_0$ state in Eu^{3+} ion. In the excitation spectrum of $NaGdF_4$:Pr,Eu, one can see the excitation peak at around 180 nm, assigned to the *f-d* transition in Pr^{3+} ions.

These results show clearly that the VUV light absorption in Pr^{3+} ions gives the red luminescence of Eu^{3+} ions. It is concluded that the energy transfer from Pr^{3+} ions to Eu^{3+} ions through Gd^{3+} sublattice efficiently occurs in $NaGdF_4$:Pr,Eu. Further study is needed to confirm whether the "quantum cutting" occurs or not in this system.

References

[1] R.T. Wegh, H. Donker, K.D. Oskam and A. Meijerink, Science **283** (1999) 663.
[2] H.S. Kiliaan, J.F.A.K. Kotte and G. Blasse, Chem. Phys. Lett. **133** (1987) 425.
[3] J.L. Sommerdijk, A. Bril and A.W. de Jager, J. Lumin. **8** (1974) 341.

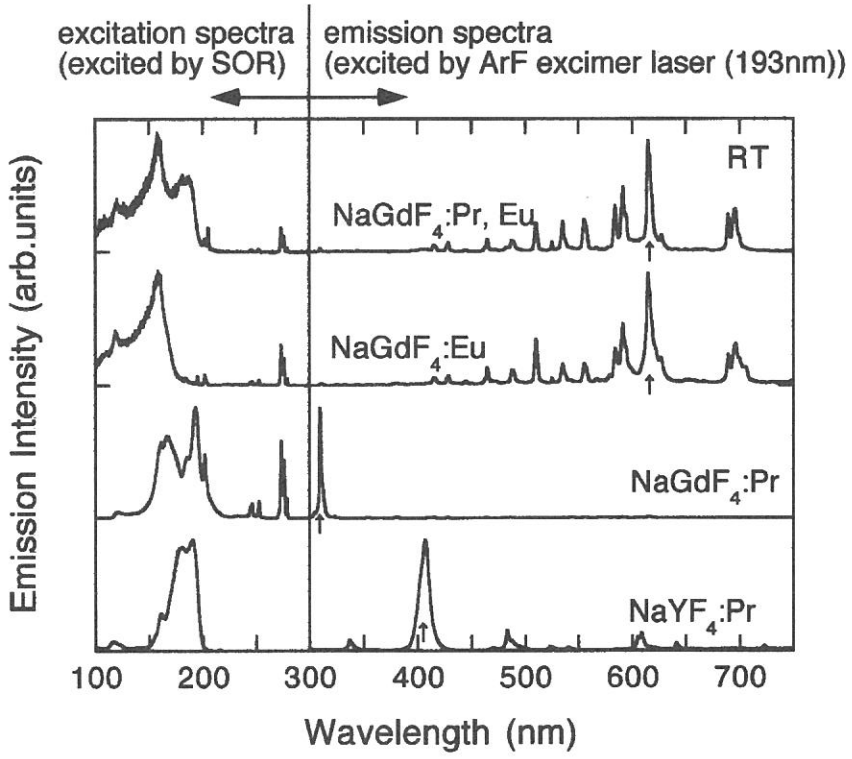

Figure 1. Luminescence spectra excited by 193-nm ArF excimer laser (right) and the excitation spectra for the luminescence lines indicated by arrows (left) at room temperature.

(BL1B)

Study on the defects in silica irradiated by a nuclear reactor

Tomoko Yoshida[1], Tetsuo Tanabe[1], Tatsuya Ii[2], Shunsuke Muto[1] and Yoshitaka Inaki[3]

[1]*Center for Integrated Research in Science and Engineering, Nagoya University, Nagoya 464-8603, Japan*

[2]*Department of Nuclear Engineering, Graduate School of Engineering, Nagoya University, Nagoya 464-8603, Japan*

[3]*Department of Applied Chemistry, Graduate School of Engineering, Nagoya University, Nagoya 464-8603, Japan*

Introduction

Neutron irradiation and radiation effects on silica glasses are one of the main concerns for their application as optical windows, insulators and optical fibers in fusion reactors as well as fission reactors.[1,2] Recently, dynamic effects of the irradiation in silica glasses have been observed as degradations of their good transparency, high electrical resistivity, low optical absorption and luminescence during in-reactor irradiation.[1-5] In order to investigate dynamic effects of in-reactor irradiation on silica, we have tried to make in situ luminescence measurement of silica glasses induced by in-reactor irradiation. In-reactor luminescence (IRL) was expected to originate mainly from the defects in silica. To confirm this, in the present study, IRL was compared with the photoluminescence which would be closely correlated to the defects in silica.

Experimental

The samples used in this work were fused silica glasses (T-1030 and T-2030) and synthesized silica glasses (T-4040) of 13 mm diameter and 2 mm thickness produced by Toshiba Ceramics, Japan with different OH content.

In-reactor irradiation have been carried out using the nuclear reactor YAYOI at the University of Tokyo. YAYOI was operated with a power of 0.5 or 1.5 kW (the neutron flux were about 2×10^{15} n/m^2 s and 6×10^{15} n/m^2 s, respectively) with an average neutron energy of 1.3 MeV and γ ray level was about 3.0 kGy/h.[6]

The photoluminescence (PL) spectra were measured at room temperature using synchrotron radiation at the beam line 1B station (BL-1B) attached with an 1m Seya-Namioka monochromator at UVSOR, Institute for Molecular Science, Okazaki, Japan, operated at electron energy of 750 MeV. The spectra were measured using monochromator (SPEX 270M) equipped with a photomultiplier (Hamamatsu R4220).

Results and Discussion

Fig. 1 shows observed luminescence spectra from various types of silica glasses irradiated in the reactor core. One can see that the IRL spectra of the low-OH fused silica glass (T-2030) consist of two broad bands peaked at 4.2 and 3.1 eV. The intensity of the 4.2 eV IRL band stayed constant during irradiation, while that of the 3.1 eV IRL band decreased linearly with the irradiation time. The high-OH fused silica glass (T-1030) showed similar double peaked spectra but the emission intensity was much less than that for the low-OH fused silica glass (T-2030). The 4.2 eV IRL band also showed no change with the irradiation time, whereas the other IRL band was centered at 2.8 eV not at 3.1 eV, and grew with the irradiation. For the high-OH synthesized silica glass (T-4040), the IRL band at the lower energy side can not be seen in Fig. 1. However, a new IRL band appeared at 2.8 eV and its intensity increased by the prolonged irradiation

Fig. 2 shows the photoluminescence (PL) spectra obtained under excitation at various energy (5.1 eV - 7.7 eV) for both the low-OH fused silica glass (T-2030) and the high-OH synthesized silica glass (T-4040) before and after the irradiation. In the spectrum of the unirradiated low-OH fused silica (Fig. 2a), two PL bands at 3.1 eV and 4.2 eV were observed, and these two PL bands were reduced remarkably by the in-reactor irradiation (Fig. 2b), which is parallel to the 3.1 eV IRL band. On the other hand, the PL spectra of the unirradiated high-OH synthesized silica glass (T-4040) were different from those of the low-OH one (T-2030); no significant PL

band was observed (Fig. 2c). After the in-reactor irradiation, two new PL bands at 2.8 eV and 4.3 eV appeared. This is again parallel to the 2.8 eV IRL band. These results suggest that the origins of the present IRL and PL would be the same.

Thomon *et al.*[7] reported the existence of two B_2 bands excited at 5.1 eV, and it is commonly accepted that the PL emission bands at 2.7 eV and 4.4 eV are attributed to the $B_{2\alpha}$ while the $B_{2\beta}$ center generates the 3.1 eV and 4.2 eV PL bands. Therefore, the PL and IRL bands for the low-OH fused silica glass (T-2030) and the high-OH synthesized silica glass (T-4040) are very likely originate from the different two types of oxygen deficiencies, $B_{2\beta}$ and $B_{2\alpha}$ centers, respectively.

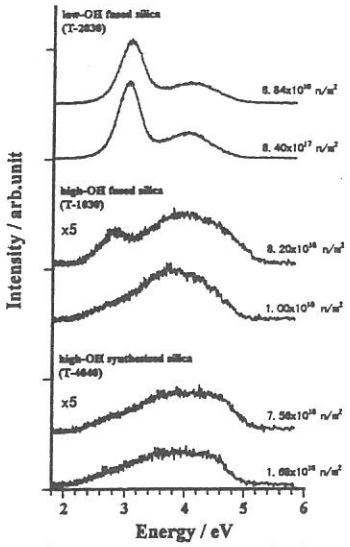

Fig.1 Luminescence spectra of silica glasses during the irradiation in the reactor core.

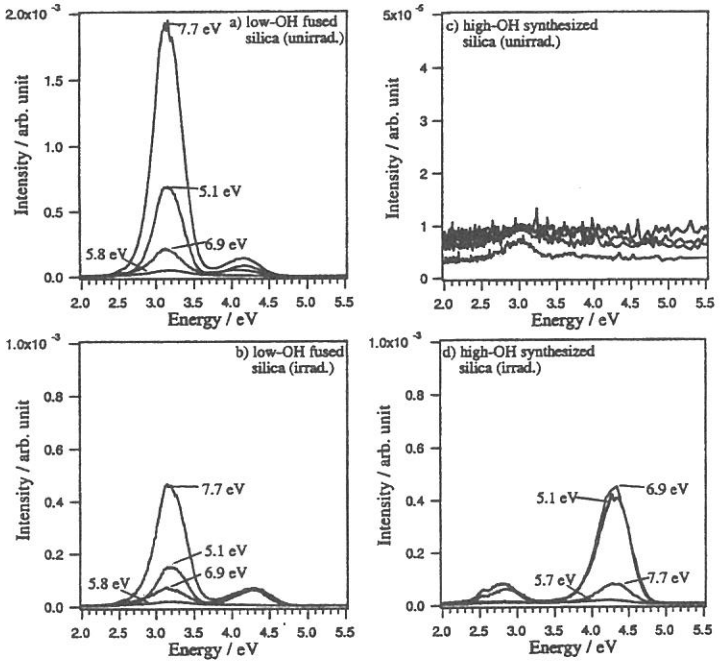

Fig. 2 The photoluminescence emission spectra excited at various energies in (a) an unirradiated low-OH fused silica glass (T-2030), (b) the reactor irradiated low-OH fused silica glass (neutron fluence is 2.8 x 10^{19} n/m^2), (c) an unirradiated high-OH synthesized silica glass (T-4040), and (d) the reactor irradiated high-OH synthesized silica glass (neutron fluence is 2.7 x 10^{20} n/m^2). The excitation energies are shown in the figure. The excitation energies in (c) are the same as those in (d).

References

[1] F. W. Clinard, Jr and L.W. Hobbs, Physics of Radiation Effects in Crystal (Elsevier, Amsterdam, 1986) p. 442.

[2] Proc. US/Japan Workshop on Dynamic Effects of Irradiation in Ceramics, Santa Fe, November 11-14,1992, Los Alamos National Laboratory Report LA-UR-92-4400 (1992)

[3] E. H. Farnum et al., J. Nucl. Mater. 191/194 (1992) 548.

[4] E. R. Hodgson, J. Nucl. Mater. 191/194 (1992) 552.

[5] T. Shikama et al., J. Nucl. Mater. 191/194 (1992) 544 and 575.

[6] M. Nakazawa and A. Sekiguchi, Radiation Dosimetry Data for Reactor YAYOI, Interior, Report of University of Tokyo, R0037 in Japanese.

[7] R. Tohmon, H. Mizuno, Y. Ohki, K. Sasagane, K. Nagasawa and Y. Hama, Phys. Rev. B 44 (1989) 1337.

(BL1B)

Vacuum-ultraviolet reflectance spectroscopy of transition-metal oxides

Katsuhiro TOBE [1], Yasujiro TAGUCHI [1], Kyoko ISHIZAKA [1], Shigeki MIYASAKA [2], Takafumi SAITO [3], Taka-hisa ARIMA [3], and Yoshinori TOKURA [1,2]

[1] *Department of Applied Physics, University of Tokyo, Tokyo 113-8656*

[2] *Joint Research Center for Atom Technology (JRCAT), Tsukuba 305-0046*

[3] *Institute of Materials Science, University of Tukuba, Tsukuba 305-8573*

One of the most important characteristics for the correlated electron systems is the drastic re-construction of electronic structure over an energy scale of eV with changes of temperature, doping concentration, and/or external field. Optical reflectivity measurements over a wide energy range and the optical conductivity spectra derived from the reflectivity spectra provide us with useful information about the strongly correlated electron systems.

In this beam time, we measured the reflectivity spectra of several transition-metal oxides, including Mn-, Ni-, Co-, Mo- and V-oxides, for an energy range of 4 eV < E < 35 eV at room temperature using the beam line BL1B. The measured reflectivity data, together with the lower-energy data below 6 eV, were used to derive the optical conductivity spectra or dielectric function via the Kramers-Kronig analysis. As an example, the imaginary part of the dielectric function of perovskite-type Mn-oxide, a detwinned single crystal of $LaMnO_3$ is shown below. This compound shows the orbital ordering below $T_{oo} \sim 780$ K.

At the orbital-ordered state, the spectra show the strong anisotropy between the polarizations parallel and perpendicular to the *c*-axis in the *Pbnm* orthorhombic structure. These polarization-dependent optical spectra are interpreted in terms of anisotropic electronic structure reflecting orbital ordering. Since the anisotropy is especially pronounced for a peak at 8 eV, this peak is assigned to the transition between O 2*p* and Mn e_g levels.

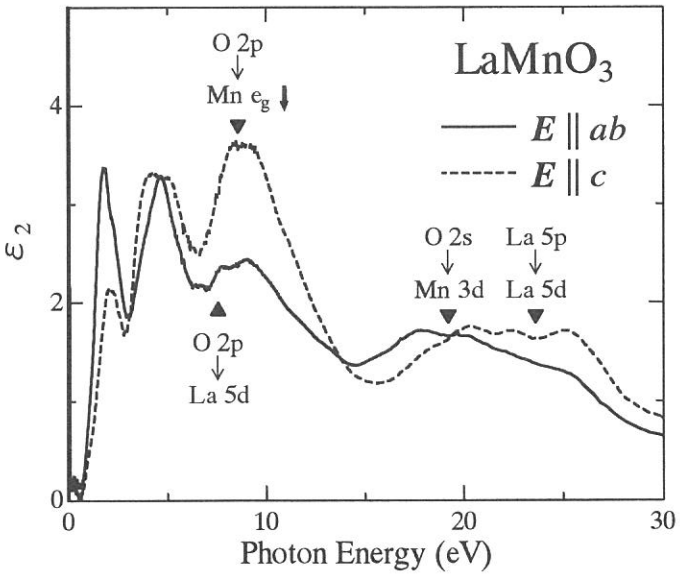

(BL6A1)

Study of Secondary Battery Substances $Li_{1-x}NiO_2$ by Millimeter Wave Reflection Measurements

Hitoshi Ohta, Yuichi Miura, Kenji Hazuki, Takao Nanba[A], Atushi Hirano[B] and Ryoji Kanno[B]

Department of Physics, Faculty of Science, Kobe University, 1-1 Rokkodai, Nada, Kobe 657-8501
[A]The Graduate School of Science and Technology, Kobe University, 1-1 Rokkodai, Nada, Kobe 657-8501
[B]Department of Chemistry, Faculty of Science, Kobe University, 1-1 Rokkodai, Nada, Kobe 657-8501

As $LiNiO_2$ is a promising material for the positive electrode of the Li ion secondary batteries, it attracted much interest. We found the drastic increase of the reflection of $LiNiO_2$ above 300 K in the millimeter wave region previously [1, 2], and we suggested that this increase of reflection is related to the motion of Li ion in the system. Moreover, we extended our study to the low energy region down to 5 cm^{-1} and also extended our study to the study of $Li_{1-x}Ni_{1+x}O_2$ in order to discuss the effect of the non-stoichiometry, which degrades the charge and discharge characteristics [3-5]. However, the study of $Li_{1-x}NiO_2$ is important because it is the intermediate state in the charging and discharging proccesses. Thereofre, we performed the reflection measurement of $Li_{1-x}NiO_2$ in the millimeter wave region.

The reflection measurements of $Li_{1-x}NiO_2$ sample have been performed in the spectra region from 10 to 60 cm^{-1} using the beam line BL6A1 of UVSOR. The temperature was changed from 79 to 380 K. The gold plate was used as a reference and InSb detector was used as a detector. Figure 1 shows our results for $Li_{1-x}NiO_2$ sample. The reflection spectra above 25 cm^{-1} are similar with those for stoichiometric $LiNiO_2$ for all temperatures. However, the reflection spectra of $Li_{1-x}NiO_2$ below 25 cm^{-1} decrease as the temperature is increased above 300 K. This suggests the change of the motion of Li ions at high temperature in $Li_{1-x}NiO_2$. These behaviors are completely different with those of non-stoichiometry samples. For more detailed discussion, the measurements of $Li_{1-x}NiO_2$ in the lower wavenumber region below 10 cm^{-1} are required.

[1] H. Ohta *et al.*: UVSOR Activity Report 1996 (1997) 182.
[2] H. Ohta *et al.*: to appear in Jpn. J. Appl. Phys. (2001).
[3] H. Ohta *et al.*: UVSOR Activity Report 1997 (1998) 128.
[4] H. Ohta *et al.*: UVSOR Activity Report 1998 (1999) 158.
[5] H. Ohta et al.: UVSOR Activity Report 1999 (2000) 93.

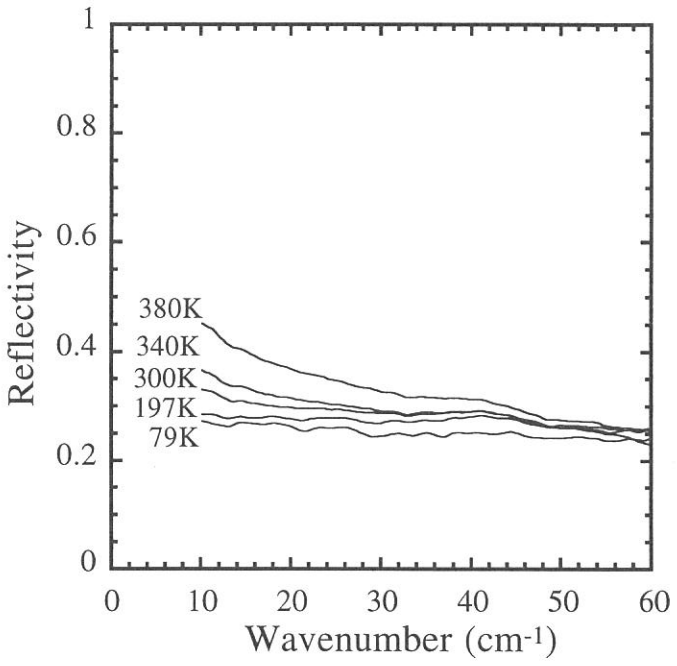

Fig. 1 Reflection spectra of $Li_{1-x}NiO_2$.

(BL5B)

Total Photoyield Spectra of Amorphous Chalcogenide Films in the VUV region

Koji HAYASHI, Yukihiro NAITO and Satoshi NAKAMURA

Department of Electrical and Electronic Engineering, Gifu University, Gifu 501-1193, JAPAN

Today, the natural environment is protected , and to ensure the safe and clean energy resource is the very important problem which must urgently reach solution. The solar cell can solve this problem, and it will be necessary energy supply source in the next generation. At present, there are crystal, polycrystal and amorphous semiconductor as a material of the solar cell. The amorphous semiconductor is the most advantageous material compared to other materials in respect of conversion efficiency and manufacture cost and area expansion, etc. Though the amorphous solar cell had been used as batteries such as electronic calculator and clock practically, the degradation by the light is large problem, when the high power was produced. However, the mechanism of the photodegradation phenomenon[1] is unresolved still. It is known that the amorphous semiconductor shows the photoinduced phenomena which is also very various except for the photodegradation phenomenon[2,3]. The application of the amorphous material to optical function devices is greatly expected by this fact. Although a large number of studies have been made on the photoinduced phenomena, there is seldom a photoinduced phenomenon in which the mechanism is clarified as well as the photodegradation phenomenon. Then, we advance the research on the photoinduced phenomena of the amorphous semiconductor using the synchrotron orbital radiation as a trial of the new research recently. Until now, these phenomena have been studied by exciting and producing the most outer shell electron using the light with the energy which corresponds to optical band gap as a light source. Using the synchrotron orbital radiation, we advance the research from the viewpoint of two. One is a viewpoint of the research of the photoinduced phenomena by the core electronic excitation, and it is a viewpoint of studying the energy structure change over the wide energy region in another. From such viewpoint, the experiment was advanced in the UVSOR facility of the Institute for Molecular Science in Okazaki, and the reversible change of optical band gap was found as a core electronic excitation effect, and it was found that the efficiency of the phenomenon depended on the energy of the exciting light[4,5]. In our recent study, we observed interesting photoinduced change in the photoconductivity and the total photoyield of amorphous chalcogenide films by the irradiation of the VUV light[6-8]. In the previous work, we measured the total photoyield spectra and the VUV reflection spectra in amorphous arsenic sulfide (a-As_2S_3) films in order to study the photoinduced effects of those optical spectra by the irradiation of the bandgap light and the VUV light[9]. In the present work, we measured the total photoyield spectra and the VUV reflection spectra in amorphous arsenic selenide (a-As_2Se_3) films.

Samples used for those measurements were amorphous chalcogenide (a-As_2Se_3 & a-As_2S_3) films. Thin films of amorphous chalcogenide were prepared onto quartz substrates by conventional evaporation technique. For the measurement of the total photoyield spectra, the amorphous chalcogenide film was deposited, after an Al electrode was fabricated on the substrate. A typical thickness of an amorphous film was around 0.5 μm. The samples were annealed at near the glass transition temperature for two hours in a vacuum. The experiments were performed at room temperature at the BL5B beam line of the UVSOR facility of the Institute for Molecular Science. For the measurement of the total photoyield spectra, we obtained the spectrum by measuring the sample drain current. We also monitored the spectrum of light source by measuring the photoyield of the gold mesh. For the measurement of the reflection spectra, the incident angle was near normal to the sample surface and the reflectivity was measured by a silicon photodiode. The reflection spectrum was obtained by normalizing the spectrum by the spectrometer system response. In the measurement of these spectra, the spectra in the equal position of the sample would be able to be measured at the same time.

Figure 1 shows the total photoyield spectra of a-As_2S_3 and a-As_2Se_3 at room temperature in the wavelength region between 15nm and 35nm. In the figure, the photoyield spectrum of the gold mesh is also shown. Two main peaks were observed at this wavelength region. One peak around 22nm corresponds to the 3d core level of Se atom. Another peak around 28nm corresponds to the 3d core level of As atom. Though these peak were also observed at the reflection spectra,

there is slight difference in the peak position. As you see in the figure, the components of the photoyield of the aluminum electrode were included for the photoyield spectra of the amorphous chalcogenide films. It is a problem to remove the components of the electrode from the photoyield spectra. In addition, there was the case in which the peak which corresponds to the core level appeared as a dip at some spectra of a-As_2S_3 films. In the measurement of the present photoyield spectra, it seems to have to consider the influence by the absorption in the thick film with not good conductivity. This point is carrying out the examination at present. Further analysis of these spectra is now in progress. We pay attention to the photoinduced effects near this wavelength region. We now are investigating photoinduced change on these spectra. The detailed experiments and analysis will be done in the next step.

This work was partly supported by grants-in-aid for Scientific Research from the Ministry of Education, Science and Culture of Japan.

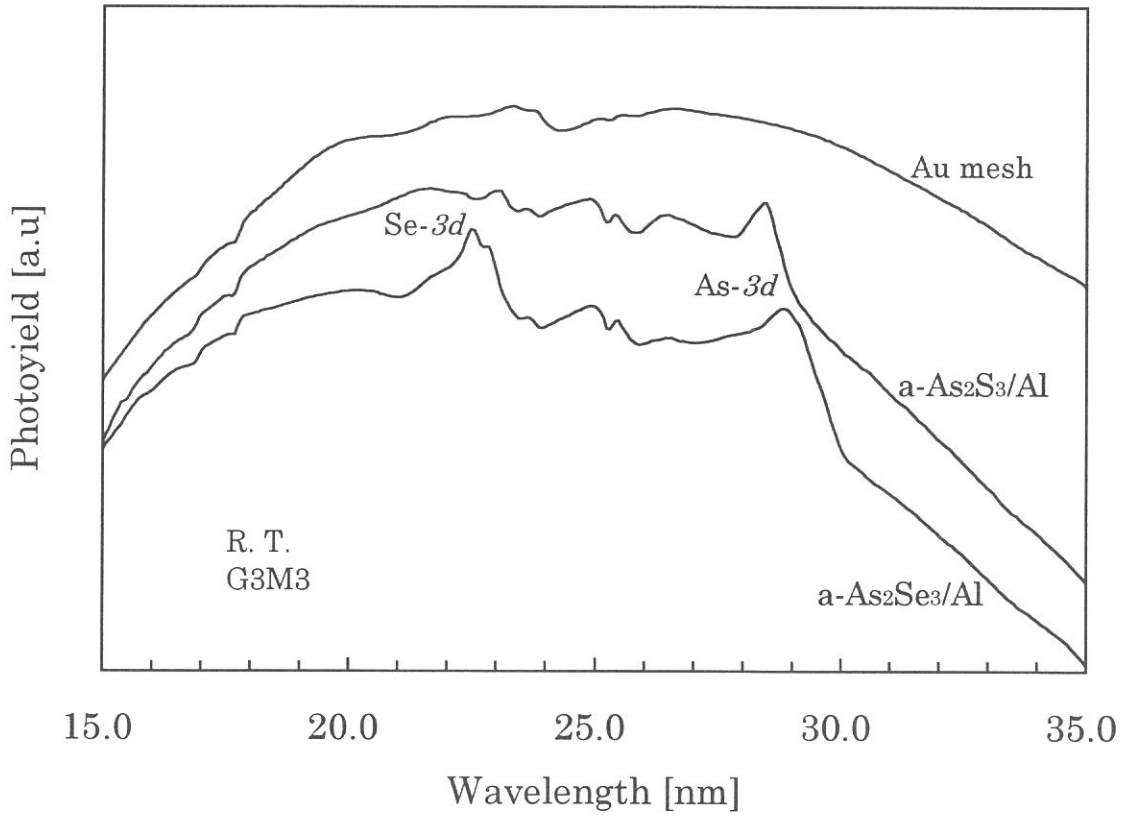

Fig. 1 Total photoyield spectra of a-As_2Se_3/Al, a-As_2S_3/Al and Au mesh at room temperature.

REFERENCES

[1] D. L. Staebler and C. R. Wronski, Appl. Phys. Lett. 31(1977)292.
[2] Ke. Tanaka, Rev. Solid State Sci., 4(1990)641.
[3] K. Shimakawa, A. Kolobov, and S. R. Elliott, Adv. Phys., 44(1995)475.
[4] K. Hayashi, D. Kato, and K. Shimakawa, UVSOR Activity Report 1995(1996)128.
[5] K. Hayashi, D. Kato, and K. Shimakawa, J. Non-Cryst. Solids., 198-200(1996)696.
[6] K. Hayashi, A. Hirai, and K. Shimakawa, UVSOR Activity Report 1996(1997)116.
[7] K. Hayashi, UVSOR Activity Report 1997(1998)118.
[8] K. Hayashi, UVSOR Activity Report 1998(1999)105.
[9] K. Hayashi, UVSOR Activity Report 1999(2000)90.

(BL5B), (BL8B1)

Development of Magnetic Kerr Rotation Apparatus in the 50-70 eV Region

K. Saito, M. Igeta, T. Ejima, T. Hatano and M. Watanabe

Research Institute for Scientific Measurements, Tohoku University
Katahira 2-1-1, Aoba-ku, Sendai 980-8577

A magnetic Kerr rotation apparatus in the 50-70 eV region has been developed. The schematic illustration is shown in Figure 1. It consists of an Al/YB_6 transmission multilyer polarizer, a magnetic circuit, a sample holder and a rotating analyzer unit. It was accommodated in a vacuum chamber equipped with a goniometer, at BL5B of the UVSOR Facility. The magnetic circuit was composed of four Sm-Co permanent magnets which generate a magnetic field of 0.82 T at a sample position. Angles of incidence of 60°-85° and 10°-30° can be chosen for longitudinal and polar Kerr configurations, respectively. A rotating analyzer unit consists of an Al/YB_6 reflection multilayer analyzer, a micro-channel plate and a pulse motor. It can be rotated around an optical axis with a fixed angle of incidence called quasi-Brewster angle. The Al/YB_6 multilayer polarizer and analyzer are similar to those employed in previous Faraday rotation measurements.[1)]

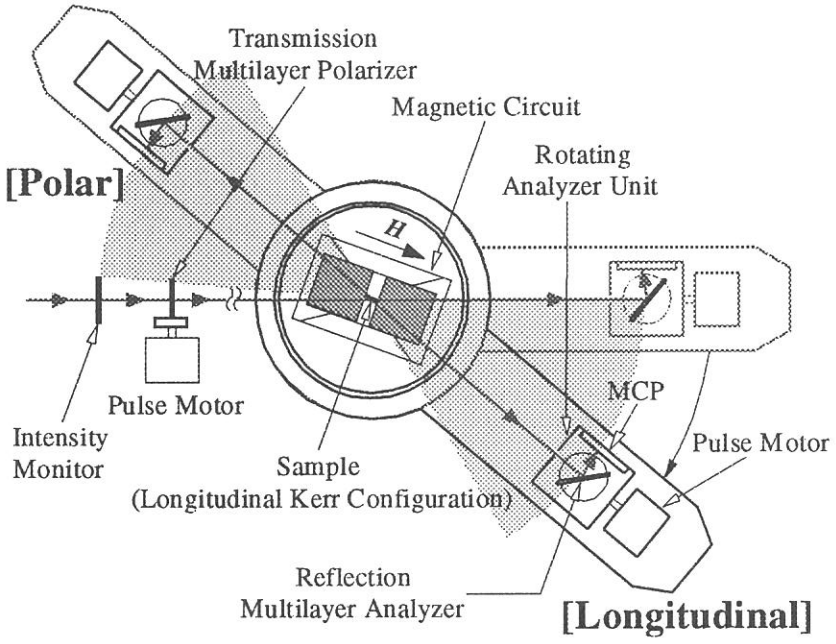

Fig. 1. Magnetic Kerr rotation apparatus.

Employing the apparatus, preliminary measurements of magnetic Kerr rotation were performed on a Co 100 nm thick single layer sputtered on a Si wafer, around Co $M_{2,3}$ absorption edges. The measurements were carried out at room temperature in longitudinal Kerr configuration in which magnetization was parallel to both the sample plane and the plane of incidence, using s-polarized incident light. Angles of incidence were fixed at $\theta = 65°$ and 80°. The experimental results for $\theta = 65°$ and 80° were plotted by closed circles in Figures 2(a) and 2(b), respectively. The maximum rotation angles about 2.5° for $\theta = 65°$ and 1.6° for $\theta = 80°$ were observed at neighborhood of Co $M_{2,3}$ absorption edges as seen in Figures 2(a) and 2(b). For the purpose to confirm the validity of the obtained Kerr rotation spectra, we have compared with those calculated from a Faraday rotation spectrum using equations derived by Zak *et al.* for determining magneto-optic coefficients.[2)] The Faraday rotation spectrum had been measured on a 39.8 nm thick Co film magnetized perpendicular to the sample plane,

in a magnetic field of 0.82 T generated by the same magnetic circuit, at BL8B1 of the UVSOR. In this calculation, we have adopted isotropic optical constants of the nonmagnetized Co film and the nonmagnetic Si wafer, given in a literature.[3] In Figures 2(a) and 2(b), calculated Kerr rotation spectra are shown by solid lines. Calculated results show that the maximum rotation angle is larger for θ = 65° than for θ = 80°, which is consistent with experimental results. However, absolute values of experimental Kerr rotation angles are smaller than those of calculated ones. The main reason for the difference may be due to the difference of magnetization between Kerr and Faraday measurements. In applied magnetic field of 0.82 T, the magnetization of the Co film is saturated in longitudinal Kerr configuration but unsaturated in the Faraday configuration. To confirm the above-mentioned reason we are carrying out the similar measurement on Ni film, of which perpendicular saturation magnetic field is 0.61 T and smaller than the applied magnetic field of 0.82 T.

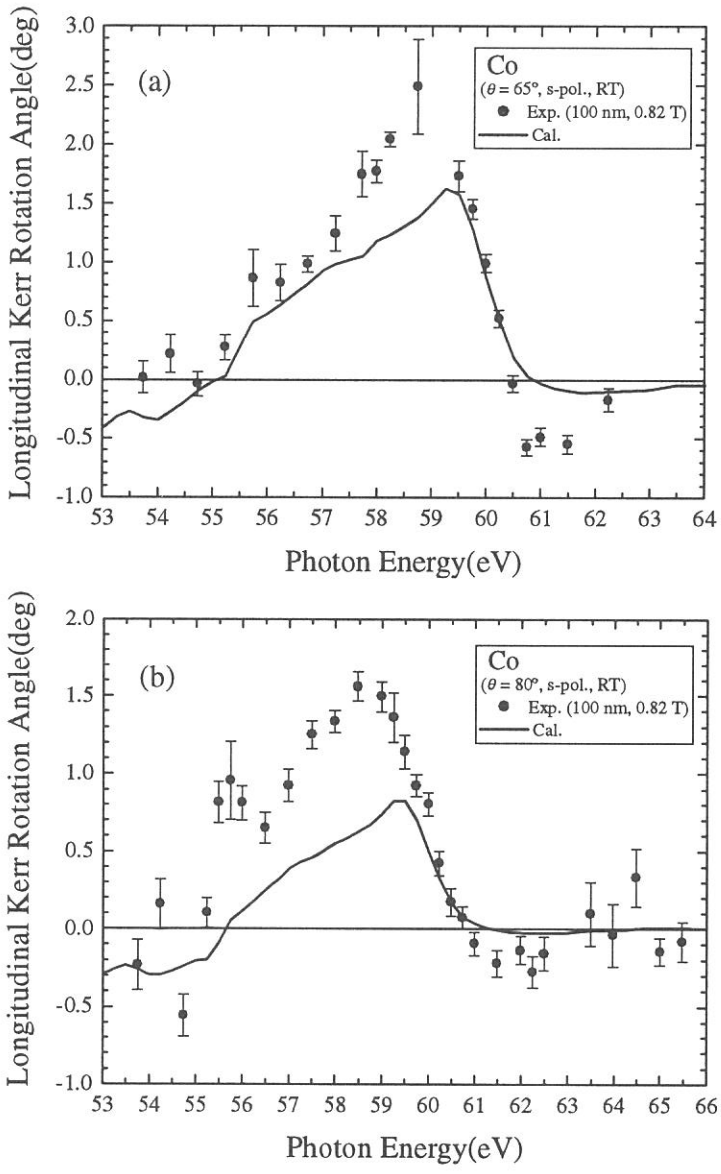

Fig. 2. Experimental (closed circles) and calculated (solid lines) longitudinal Kerr rotation spectra of Co for s-polarized light at angles of incidence of (a) θ = 65° and (b) θ = 80°.

References

1) W. Hu, T. Hatano, M. Yamamoto and M. Watanabe, J. Synch. Rad. **5** (1998) 732.
2) J. Zak, E. R. Moog, C. Liu and S. D. Bader, Phys. Rev. **B 43** (1991) 6423.
3) E. D. Palik: *Handbook of Optical Constants of Solids* (Academic Press, 1985).

(BL5B)

Reflection spectra of $Ga_{1-x}In_xN$ ternary alloy semiconductors

A. Wakahara, T.Misaki, T.Nakajima, and Q. Guo *

Toyohashi University of Technology, Tempaku-cho, Toyohashi, 441-8580, Japan
**Saga University, Saga, Japan*

Group-III nitride semiconductors, such as AlN, GaN, InN, and its alloy, have been paid much attention for application to optoelectronics, those are able to cover from 6.2 to 1.9eV. Recent progress on crystal growth achieved high quality GaN layer on sapphire substrate, and very bright blue/green light-emitting diodes (LEDs) have been commercialized, and also, continuous wave operation of current-injection violet laser has been achieved by means of GaInN/GaN multi-quantum well (MQW) laser structure [1-3]. In order to design the device structure, it is important to know fundamental properties of the materials. However, the fundamental properties of GaInN, such as effective masses, optical constants, and elastic constants, are not well investigated. Moreover, it is difficult to grow GaInN with uniform In composition, because the covalent bond length of In-N is much linger than that of Ga-N and it leads to the phase separation phenomenon, and thus it is interested in the effect of compositional in homogeneity on te band structure of GaInN. In this study, reflection spectra are measured in infra-red to vacuum ultraviolet region and optical constants are calculated via Kramers-Kronig analysis.

GaInN ternary alloy were grown on sapphire (0001) substrate by remote-plasma enhanced organometallic vapor phase epitaxy, in which RF (13.56Mhe) discharging of N_2 generated reactive nitrogen source. The group-III precursors were trimethylgallium (TMGa) and trymethylindium (TMIn). The detailed growth conditions were described in the previous publications [4]. The substrate used in the experiments was (0001)-oriented sapphire wafer. GaInN layers were grown at 680°C. In composition 'X' of GaInN layers was determined from lattice constant measured by X-ray diffraction assuming Vegard's low, and was in the range of 0.07-1.0. The layer thickness of the GaInN layer was about 0.2μm. Reflection spectra were measured by double-beam spectrometer for the photon energy less than 6eV and by BL5A for higher than 6eV. Incident angle defined as the angle between incident light and the normal direction of the sample surface was 10 degree.

Figure 1 shows reflectance spectra of GaInN with different In composition. It can be seen in the figure, that sharp peaks are observed in the range of 2-11eV. For the reflectance of InN, peaks can be seen at 2.1, 4.8, 5.3, 7.9, ~9. 10.7, and 11.2eV, and these are well agree with previously reported value [5]. The peak position of these peaks systematically shifts as decreasing the In contents. Higher energy transition was investigated via dielectric function. The dielectric function was calculated via Kramers-Kronig analysis using reflectance spectra shown in Fig.1. Figure 2 shows the imaginary part of the dielectric function 'ε_2'. In the case of GaN, critical point structures are reported at 3.4 (E_0, $\Gamma 6 \rightarrow \Gamma 1$), 6.9 ($E_1$, critical points in close to *M*), 7.75 (*A-L* and *L-M*), and 9.2eV(*Γ-M* and *A-H*) [6]. For InN, critical point structures can be seen at 2.3, 4.7, 5.3, ~8, ~9, and ~10eV. Critical points at 2.3, 4.7, 5.3, and ~10eV would be corresponding to the transitions of E_0, $U_4 \rightarrow U_1$(critical point in *L-M*), $M_2 \rightarrow M_1$, and critical point in *Γ-M*, respectively [5,7]. In order to see the shift of critical points as a function of

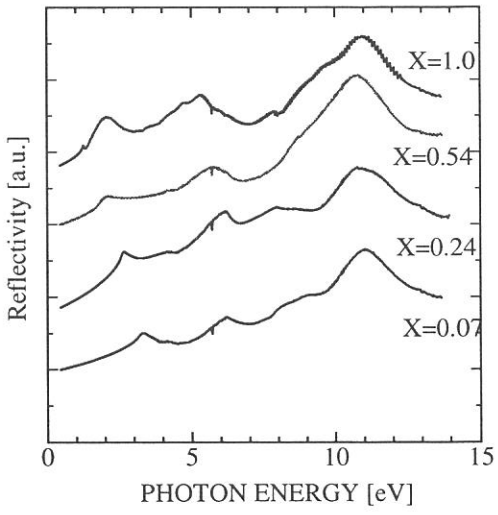

Fig.1. Reflectance spectra of GaInN with different In composition.

In composition, we focused on the peaks corresponding to the similar transitions observed in both GaN and InN. Figure 3 shows relationship between the transition energy of critical point and In composition. As can be seen in the figure, both E_0 and E_1 decrease with increasing In composition. The transition energies of E0 and E1 are well fitted to a relation of $E(x)=E_{GaN}(1-X)+E_{InN}(X)-bX(1-X)$, where X is In composition and b is called bowing parameter. Obtained bowing parameters for E_0 and E_1 transitions estimated from the figure are 1.8eV and 0.6eV, respectively. The obtained bowing parameter for E_0 transition is larger than the reported value of 1eV [8,9]. E_1 and other higher band transitions indicate small bowing.

References

1] S.Nakamura, T.Mukai, and M.Senoh, Appl.Phys.Lett. **64** (1994) 1687.

2] S.Nakamura, M.Senoh, N.Iwasa, S.Nagahama, T.Yamada, and T.Mukai, Jpn.J.Appl.Phys. **34** (1995) L1332.

3] S.Nakamura, M.Senoh, S.Nagahama, N.Iwasa, T.Yamada, T.Matsushita, Y.Sugimoto, and H.Kiyoku, Appl.Phys.Lett. **69** (1996) 4056.

4] T.Tokuda, A.Wakahara, S. Noda, and A. Sasaki, J. Crystal Growth **187** (1998) 178.

5] Q.Guo, O.Kato, M.Fujisawa, and A.Yoahida, Solid State Commun. **83** (1992) 721.

6] J.P.L.Hughec, Y.Wang, and J.E.Sipe, Phys. Rev. **B 55** (997) 13630.

7] A.Wakahara, T.Tsuchiya, and A. Yoshida, Vacuum **41** (1990) 1071.

8] K.Osamura, S.Naka, and Y.Murakami, J. Appl. Phys. **46** (1975) 3432.

9] S. Nakamura, T.Mukai, M.Senoh, S.Nagahama, N.Iwasa, J. Appl. Phys. 74 (1993) 3911.

10] S.Adachi, Optical constants of crystalline and amorphous semiconductors, Chap. B9, (Kluwer Academic Publishers, Boston,1999)

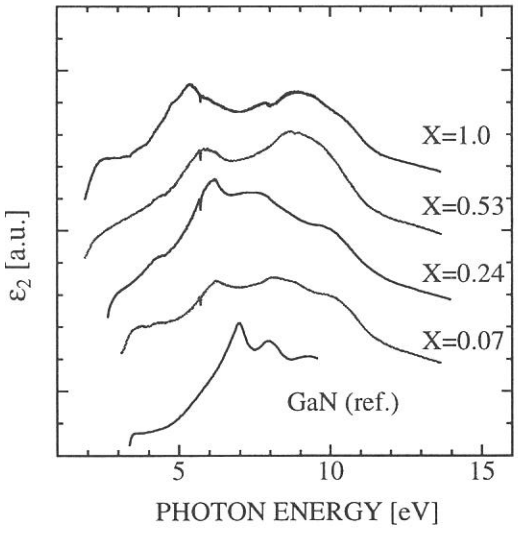

Fig.2. Change of imaginary part of dielectric function ε_2 for different In composition 'X' of GaInN. Dielectric function of GaN is taken from the literature [10].

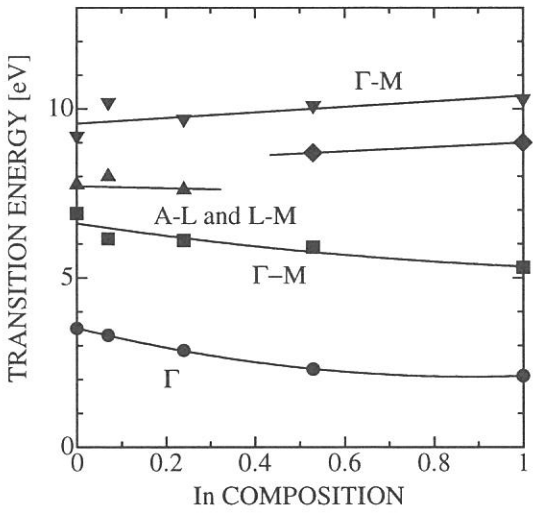

Fig.3. In composition dependence of critical points.

(BL5B, 6A1, 7B)

Spectral Range Effect to the Optical Constants via Kramers-Kronig Analysis: Reflectivity Spectrum of CeSb in the FIR-SX Region

Shin-ichi Kimura[1, 2], Mitsuru Okuno[1], Hideki Iwata[1], Hideaki Kitazawa[3] and Giyu Kido[3]

[1]*Graduate School of Science and Technology, Kobe University, Nada-ku, Kobe 657-8501*
[2]*PRESTO, Japan Science and Technology Corporation*
[3]*Physical Properties Division, National Research Institute for Metals, 1-2-1 Sengen, Tsukuba, 305-0047*

To obtain optical constants of solids, some methods are adopted. In the case of insulators, the ellipsometry that can directly measure the phase shift is a powerful tool for the investigation of the optical constants as well as the electronic structure. However, the method cannot be adapted to metallic materials because these cannot be transparent. In such case, the Kramers-Kronig analysis (KKA) is useful. The KKA needs an accurate reflectivity spectrum in the energy range from 0 to infinity. However, since we cannot measure a spectrum in such energy range, we have to extrapolate below and above the obtained spectrum. Here we report the effect of the limited energy range to the optical constants.

The reflectivity spectrum of CeSb at 300 K is measured in the energy range from far-infrared to soft x-ray (0.01 - 250 eV) by using BL6A1 (0.01 – 1.5 eV), BL7B (1.4 – 30 eV) and BL5B (15 – 250 eV) shown in Fig. 1. CeSb is one of typical strongly correlated electron systems with 4f electrons and low carrier density [1]. It is easy to cleave along a (100)-plane because of the NaCl-type crystal structure. In the BL7B and BL5B region, the clean surface of the sample was obtained by cleavage *in situ*. Because the cleavage surface is flat microscopically, no diffused scattering on the surface occurs. Then absorption peaks in the high-energy range, for instance the Ce 4d-4f absorption at 120 eV, were clearly observed.

The optical conductivity spectra of CeSb obtained by the KKA of the reflectivity spectrum are shown in Fig. 2. Three lines indicate the optical conductivity spectra using the different limited

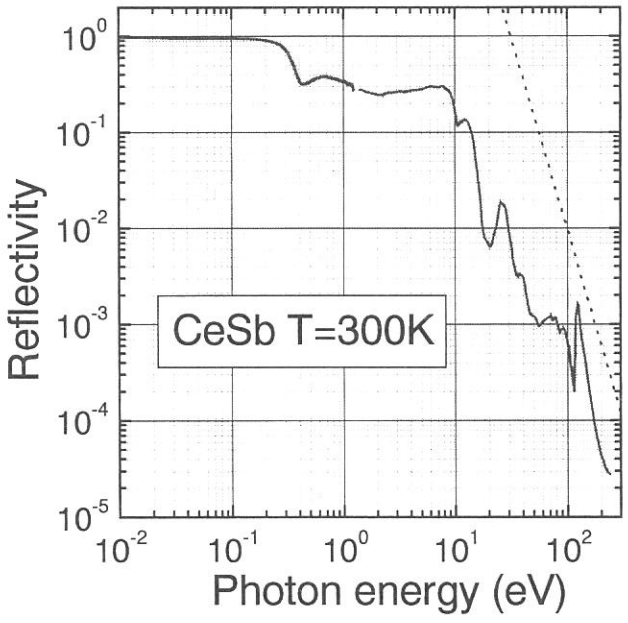

Fig. 1. Reflectivity spectrum of CeSb in the energy range of 0.01 – 250 eV at 300 K (solid line). The dotted line indicates the slope of $R(\omega) \propto \omega^{-4}$.

energy range of the reflectivity spectrum. The solid line is the energy range of 0.01 – 250 eV, the dashed line 0.01 – 30 eV (up to the BL7B and BL1B region) and the dotted line 0.01 – 6 eV (up to the conventional UV spectrometer region). The extrapolations below and above the energy range were commonly adapted to be the Hagen-Rubens function ($R(\omega) = 1 - A\cdot\omega^{1/2}$) and $R(\omega) = B\cdot\omega^{-4}$, respectively [2]. Here, A and B were determined to be smoothly connected to the reflectivity spectrum.

The solid line in Fig. 2 indicates six main structures, the absorption due to carriers below 0.3 eV, Sb 5p → Ce 5d (from the valence band to the conduction band) at 0.5 – 15 eV, Ce 5p → 5d at 25 eV, Sb 4d → 6p at 39 eV, Sb 4p → 5d at 80 eV and Ce 4d → 4f at 120 eV. The solid line is a reasonable spectrum of the electronic structure of CeSb. The dashed line is very similar to the solid line below 30 eV. However the dotted line is much different from the solid line. Particularly, the shape of the Sb 5p → Ce 5d absorption is much different because of the limitation of the energy range. In addition, the shape of the carrier absorption is different from the solid line. This causes a mistake to evaluate the character of carriers.

Since the extrapolation function of $R(\omega) = B\cdot\omega^{-4}$ seems to obey in the energy range above 20 eV roughly as shown in Fig. 1. The 20 eV is the upper limit of the transition from the valence band to the conduction band. The energy is almost equal among all materials. Therefore, if we use the extrapolation function of $R(\omega) = B\cdot\omega^{-4}$, the reflectivity spectrum should be measured in the energy range above 20 eV.

---

[1] T. Suzuki, JJAP Series 8 (1993) 267.
[2] F. Wooten, *Optical Properties of Solids*, Academic Press, (1972).

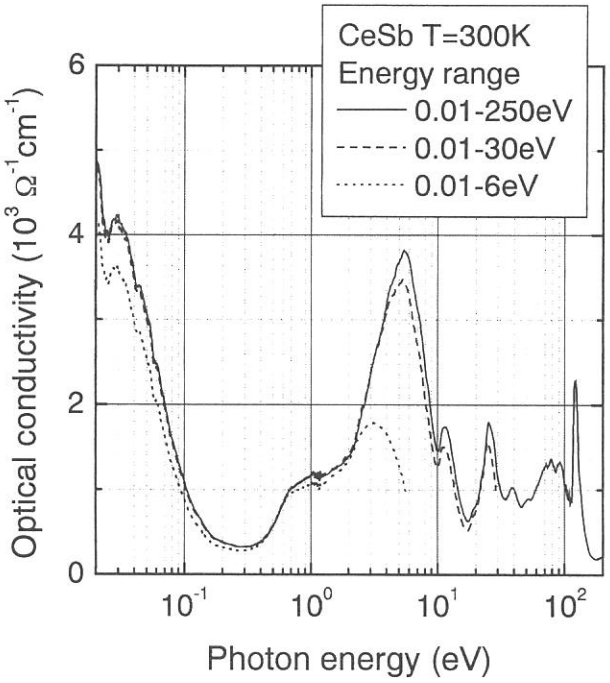

Fig. 2. The difference of the optical conductivity spectra of CeSb due to the spectral range effect. The solid line is used the reflectivity spectrum of 0.01 – 250 eV, the dashed line of 0.01 – 30 eV and the dotted line of 0.01 – 6 eV. The extrapolation functions below and above the spectral range for the Kramers-Kronig analysis were commonly adopted to be the Hagen-Rubens function and $R(\omega) = B\cdot\omega^{-4}$, respectively.

(BL6A1)

Optical conductivity spectra of Pr Ru_4P_{12} due to metal-insulator transition

Lin Chen[2], Masaya Nakayama[a], Takao Nanba[a], Itimin Shirotani[b], and Chihiro Sekine[b]

a Graduate school of Science and Technology, Kobe University, Nada-ku, Kobe 657-8501, Kobe,Japan

b Muroran Institute of Technology, 27-1, Mizumoto,Muroran 050-0071, Japan

$PrRu_4P_{12}$ are ternary metal phosphides with the skutterudite structure ($CoAs_3$-type), which is represented as RT_4P_{12} (R=rare earth element and T=transition metal). $PrRu_4P_{12}$ was found to show a metal-insulator (M-I) transition at Tc=60K [1]. After the success of the synthesis of these compounds, many kinds of experiments has started because its very attractive physical properties. In general, infrared spectroscopy is a useful tool to know the information about the precise change in the electronic structure very close to the Fermi level. The optical measurements ,however, has not yet been done for these materials. We measured the temperature dependence of the optical reflection spectra of RRu_4P_{12} (R=La,Ce,Pr and Sm) in the energy region of 0.005 -4 eV. The optical conductivity spectrum ($\sigma(\omega)$) was obtained from a Kramers-Kronig transformation of the reflectivity spectrum by using each extrapolation function at the both side of the measured spectrum[2].

Figs.1 show the temperature dependence of the low energy part of the obtained optical conductivity spectra of $PrRu_4P_{12}$. We can see that the formation of the shoulder-like structure takes place around 0.04 e V at the low temperature regions instead of the disappearance of the Drude part due to the collective motion of the free carriers in the conduction bands at the higher temperatures. This means that the energy gap was formed with the magnitude of 0.04 eV at 10 K. The position of the shoulder shifts slightly towards the lower energy-side as well as the suppression of the gap by the Drude component according to the increase in the temperatures.

Fig. 2 shows the obtained $\sigma(\omega)$ -spectra of $PrRu_4P_{12}$ at 78 and 300 K in which $PrRu_4P_{12}$ are a metallic state, and the decomposition of the low energy part to the two simple Drude components (broken curves *a* and *b*). The existences of the two Drude components in the $\sigma(\omega)$ -spectra means that there are at least two branches which come across the Fermi level. The component, *a*, corresponds to the band which has a larger Fermi surface between the two bands because the carrier concentration is higher than the component *b*. The possibility of the existence of the two bands which come across the Fermi level in the energy band scheme of $PrRu_4P_{12}$ are pointed out by the recent energy band [3].

References

[1] C.Sekine, T.Uchiumi, I.Shirotani, and T.Yagi, Phys.Rev.Lett.79, (1997)3218.

[2] T.Nanba et.al. Physica B259-261 (1999)853-854.

[3] H.Harima for a private communication.

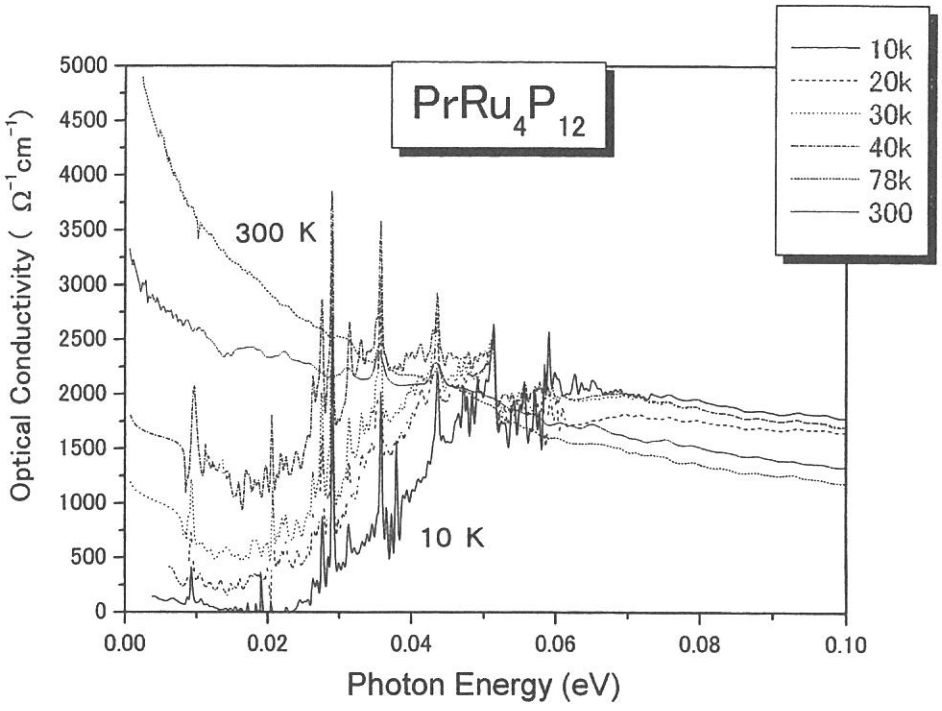

Fig.1

The temperature dependence of the low energy part of the obtained σ-spectra of $PrRu_4P_{12}$.

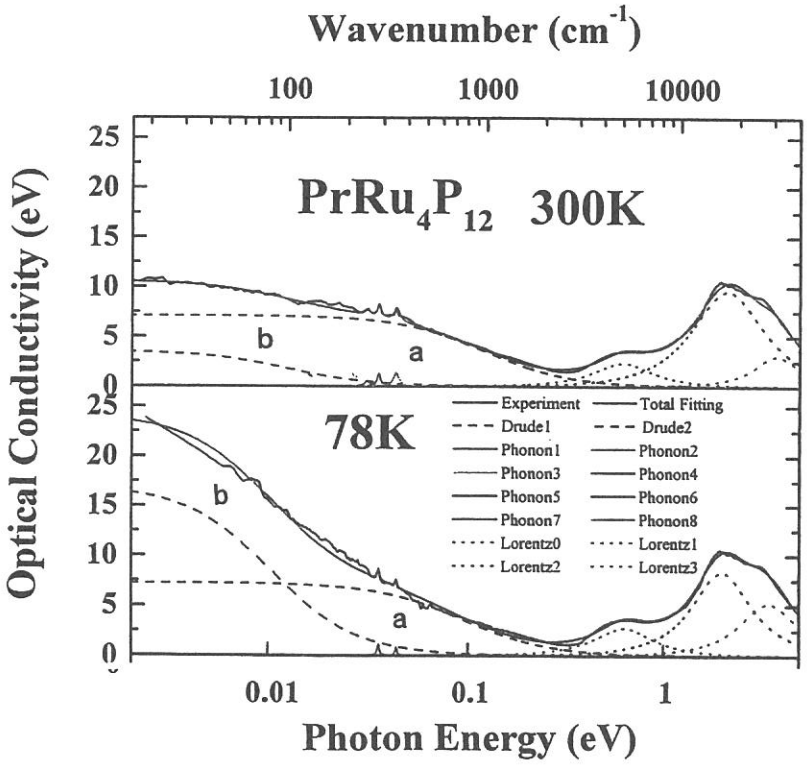

Fig.2 The σ-spectra of $PrRu_4P_{12}$ at 300 and 78 K and its decomposition of the low energy part to two Drude-terms.

(BL6A1)

Infrared absorption spectrum of GaAs

Ichiro Shoji, Sunao Kurimura and Takunori Taira

Laser Research Center for Molecular Science, Institute for Molecular Science, 38 Nishigonaka, Myodaiji, Okazaki 444-8585, Japan

Wide-tunable near-infrared (IR) to mid-IR light sources are needed for a variety of applications, including spectroscopy, chemical monitoring, biomedical applications, and atmospheric and environmental sensing. Frequency down conversion of 1 μm pump sources such as Nd:YAG lasers using optical parametric oscillation or difference-frequency generation is a promising approach to obtain coherent light in the IR region. Since it is necessary to satisfy the phase-matching condition between the pump, signal, and idler light in order to realize high conversion efficiency, the conventional phase-matching method using birefringence in nonlinear-optical crystals limited the wavelength range and materials applicable. On the other hand, quasi-phase matching (QPM) technique which periodically modulates the magnitude of the nonlinear-optical coefficient has many advantages and has been intensively studied. Especially, recent developments in fabrication of periodically poled $LiNbO_3$ (PPLN) [1] have realized high-power pulse and cw optical parametric oscillators which emit up to 4 μm. However, PPLN cannot be used for generating light of wavelength longer than 6 μm, because IR absorption in $LiNbO_3$ becomes significant. Although generation of mid-IR light around 10 μm region, which is often called "fingerprints region for molecules," have been made with birefringent phase matching in some compounds such as $AgGaS_2$, $AgGaSe_2$, and $ZnGeP_2$, these materials are difficult to grow, thermo-mechanically weak, and have low optical damage thresholds.

We are developing QPM devices using GaAs, which can generate mid-IR light up to ~16 μm. GaAs has a large optical nonlinearity: the nonlinear optical coefficient of GaAs is 170 pm/V at wavelength of 1.06 μm, which is more than 6 times larger than that of $LiNbO_3$ [2]. Its transparent range is as wide as 1–16 μm. Moreover, since GaAs is a popular semiconductor, the crystal-growth and processing technologies are matured enough. We are fabricating the GaAs QPM structure by the diffusion-bonding

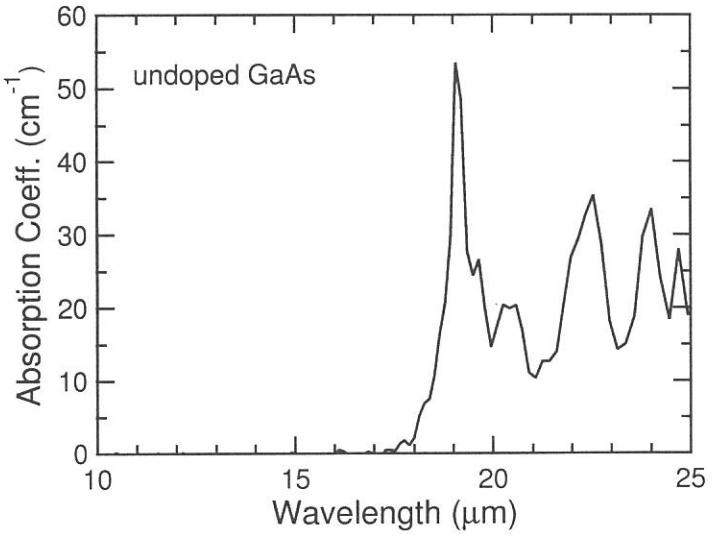

Fig 1. Infrared absorption spectrum of the undoped GaAs.

technique, in which several-tens-to-hundreds of micron-thickness GaAs plates are stacked with the directions alternatively reversed, and bonded at the atomic level by heating. Although this technique was applied first at Stanford University [3], the scattering losses at the interfaces of the plates were significant and only low conversion efficiencies were reported [4]. However, we believe that the optical loss can be greatly reduced by optimizing the fabrication processes. We report here the IR absorption spectra of a raw GaAs sample, which can be used as reference.

Absorption spectra of semiconductors strongly depend on the dopant concentration. Semi-insulating or high-resistivity samples are suitable for frequency-conversion devices because optical absorption is much lower. We have prepared an undoped GaAs sample grown by Hitachi Cable, Ltd. The resistivity was $\geq 10^7\ \Omega\,\mathrm{cm}$, the thickness 465 μm, and the both facets were optically polished. The absorption spectrum was measured with the rapid-scan Michelson FT-IR (Bruker) at the beam line BL6A1. Using the KBr beam splitter and a MCT detector, we made a measurement in the wavelength range of 1–25 μm (10000–400 cm^{-1}).

Figure 1 shows the obtained absorption spectrum. The wavelength range 1–10 μm, where no absorption was observed, is not shown. The obtained result is in agreement with previously reported spectrum of a n-type but high resistivity sample [5]. However, the absorption coefficients in low-absorption region of 12–18 μm, which are important for evaluating the performance of the QPM device, could not be accurately obtained in our measurement because of low signal-to-noise ratios. A much thicker sample should be used in order to measure such small absorption coefficients.

We have a plan to compare the absorption coefficients between the diffusion-bonded stacked sample and the raw bulk sample to evaluate the scattering losses at the interfaces of the stacked sample, and feedback the fabrication processes.

References

[1] L. E. Myers, R. C. Eckardt, M. M. Fejer, R. L. Byer, W. R. Bosenberg, and J. W. Pierce, J. Opt. Soc. Am. B **12,** 2102 (1995).

[2] I. Shoji, T. Kondo, A. Kitamoto, M. Shirane, and R. Ito, J. Opt. Soc. Am. B **14,** 2268 – 2294 (1997).

[3] L. Gordon, G. L. Woods, R. C. Eckardt, R. R. Route, R. S. Feigelson, M. M. Fejer, and R. L. Byer, Electron. Lett. **29,** 1942 (1993).

[4] D. Zheng, L. A. Gordon, Y. S. Wu, R. S. Feigelson, M. M. Fejer, and R. L. Byer, Opt. Lett. **23,** 1010 (1998).

[5] W. Cochran, S. J. Fray, F. A. Johnson, J. E. Quarrington, N. Williams, J. Appl. Phys. **32,** 2102 (1961).

(BL6A1, BL7B)

Optical reflectivity study of colossal magneto-resistance pyrochlore $Tl_2Mn_2O_7$

H. Okamura, T. Koretsune, M. Matsunami, S. Kimura, T. Nanba,
H. Imai[A], Y. Shimakawa[A], Y. Kubo[A]

Department of Physics and Graduate School of Science and Technology, Kobe University, Kobe 657-8501.
[A]Fundamental Research Laboratories, NEC Corporation, Tsukuba 305-8501, JAPAN

Physics of the colossal magneto-resistance (CMR) phenomena has been one of the central issues of condensed matter physics in the last several years. In particular, the ferromagnetic perovskite manganites, e.g., $La_{1-x}Sr_xMnO_3$, have attracted much attention [1]. More recently, the $Tl_2Mn_2O_7$ pyrochlore has been attaining increasing interest, since it exhibits a CMR that is comparable to those observed for the perovskites [2]. $Tl_2Mn_2O_7$ is also a ferromagnet, and its resistivity (ρ) drops rapidly upon cooling through $T_c \sim 120$ K. Near and above T_c, an external magnetic field of 7 T reduces ρ by a factor of ~ 10. Although these features appear very similar to those for the perovskites, various studies have suggested that the underlying mechanism should be very different from that in the perovskites [2]. In order to probe the electronic structures of $Tl_2Mn_2O_7$ and its relation to the CMR, we have studied the infrared optical reflectivity of $Tl_2Mn_2O_7$ under magnetic fields at BL6A1, and the optical reflectivity in the visible, UV, and VUV ranges at BL7B. Figure 1 shows the reflectivity spectra (R) measured at various temperatures (T) and magnetic fields (B). Figure 2 shows the optical conductivity spectra (σ) obtained from R using the Kramers Kronig relations. The sample used had a Curie temperature (T_c) of 120 K, and the T-induced spectral change is very large around T_c. In addition, the B-induced spectral changes are also largest near and above T_c (120 K - 140 K). These spectral changes show that the electronic structures of $Tl_2Mn_2O_7$ become metallic and the carrier density increases below T_c, and the same change occurs also above and near T_c in strong magnetic fields. The range 120-140 K is also where the CMR is observed, and the CMR mechanism in $Tl_2Mn_2O_7$ should be closely related to this carrier density increase.

References

[1] See, for example, Y. Tokura et al. J. Phys. Soc. Jpn. **63**, 3931 (1994).

[2] Y. Shimakawa et al., Nature **379**, 53 (1996); Phys. Rev. B **55**, 6399 (1997).

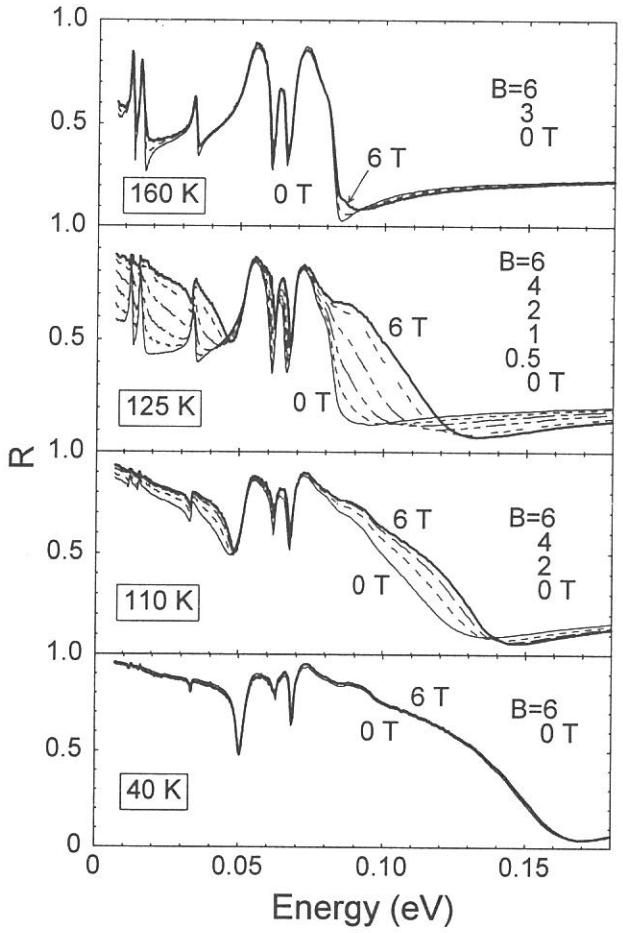

FIG. 1. Reflectivity (R) spectra of $Tl_2Mn_2O_7$ at temperatures 160, 125, 110, and 40 K in various magnetic fields (B).

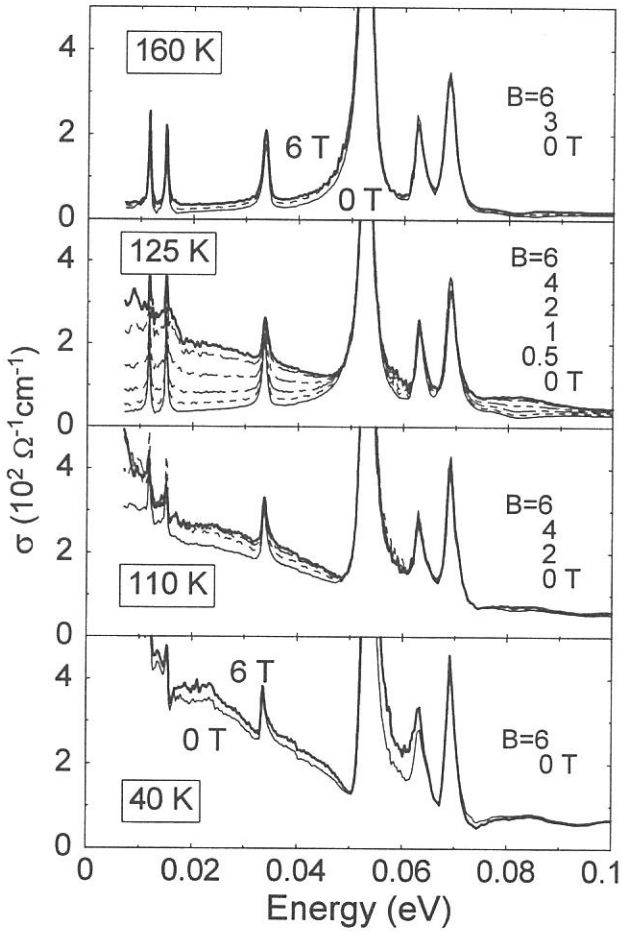

FIG.2 : Optical conductivity (σ) spectra of $Tl_2Mn_2O_7$ at temperatures 160, 125, 110, and 40 K in various magnetic fields (B).

(BL7B)

Responsivity spectra of GaN based UV detectors in VUV region

Atsushi Motogaito[1], Motoo Yamaguchi[1], Kazumasa Hiramatsu[1], Masahiro Kotoh[2], Youichiro Ohuchi[2], Kazuyuki Tadatomo[2], Yutaka Hamamura[3] and Kazutoshi Fukui[4]

[1]*Deptartment of Electrical and Electronic Engineering, Mie University, 1515 Kamihama, Tsu, Mie, 514-8507*

[2]*Photonic Research Laboratory, Mitsubishi Cable Industries, Ltd., 4-3 Ikejiri, Itami, Hyogo, 664-0027*

[3]*Sagamihara Plant, Nikon Co., Ltd., 1-10-1 Asamizodai, Sagamihara, Kanagawa, 228-0828*

[4]*Department of Vacuum UV Photoscience, Institute for Molecular Science, Myodaiji, Okazaki, Aichi, 444-8585*

The group III-nitride semiconductors are promising materials for applications in opt-electronic devices such as laser diodes and field-effect transistors. Ultraviolet (UV) detectors are one of the most attractive devices in the group III-nitride semiconductors. Now, for the measurement UV light, photodetector components with Si such as photodiodes are mainly used. However, light sensitivity often deteriorates due to radiation damage in the VUV region. Several groups have reported on GaN or AlGaN based UV detectors.

Synchrotron radiation (SR) is a powerful light source of X-ray region. However, SR is also the useful light source of V,UV – infrared (IR) region because of its wide wavelength continuity. It gives us the chances not only to investigate the electronic and optical structures, for example in ref.1) and 2), but also to characterize the responsivity spectra of UV detectors in wide wavelength region.

In this report, we describe the responsivity spectra of Schottky type UV detectors between VUV and visible (VIS) light region (λ=41-563 nm, $h\nu$=2-30 eV).

The UV detectors used in this study adopt the Schottky contacts with mesa structures. They consists of a 3 μm thick n-GaN layer ($n=2\times10^{18}$ cm^{-3}) and a 2.5 μm thick i-GaN layer ($n=1.0\times10^{16}$ cm^{-3}) on (0001) sapphire substrate. These layers are grown by metalorganic vapor phase epitaxy (MOVPE). The Au/Ni Schottky contact with mesa structure composed of 2-μm-electrode regions and 2-μm-window regions by liftoff process is deposited on i-GaN. The diameter of detectors is 6.5 mm.

The responsivity of UV detectors is estimated by measuring photo current illuminating SR at the beam line BL7B of the UVSOR Facility, Institute for Molecular Science. The BL7B is equipped with a 3m normal-incidence monochromator. The details of BL7B are already reported [3, 4]. UV detectors are illuminated with the monochromatic light, which is between $h\nu$=2.2 eV (λ=564 nm) and $h\nu$=30 eV (λ=41 nm). The measurements of photo current are performed at room temperature in the vacuum chamber under the vacuum of 10^{-9} Torr. The photo current is measured as reverse current of Schottky diode with zero bias or applying reverse bias during the illumination of SR. Responsivity of UV detectors is calculated by dividing the photo current by the photon energy.

The responsivity spectra of detectors on photon energy are measured. Figure 1 shows the responsivity spectra at zero bias. No responsivity at the energy lower than 3.4 eV (the absorption edge of GaN)

can be seen clearly. This means these detectors are available for UV or VUV region without filters, which cut off visible light. The ratio of responsivity between UV and VIS region is about 2×10^3. The characteristics of responsivity spectra are considered as follows. In the case of $h\nu$<8.0 eV, there are no photoemission current of Au and GaN so detectors can be used without photoemission. The maximum responsivity of this detector is 0.01 at $h\nu$=4.6 eV (λ=270 nm). In the case of $h\nu$>8.0 eV, photoemission currents of Au and GaN are not negligible now. Especially, $h\nu$>9.5 eV, the photoemission current of GaN, which flows in the reverse direction of photo current, is dominated so the sign of responsivity of detectors is negative. Thus, these detectors can be used between 3.4 eV (360 nm) and 8.0 eV (155 nm). There are no reports on the responsivity spectra in vacuum ultraviolet (VUV) region (λ<200 nm). Therefore this result shows that these Schottky type detectors with mesa structures are effective to detect VUV light (155<λ<200 nm).

1) O. Ambacher et al.: MRS Intern. J. Nitride Semicond. Res. 2 (1997) Article 22.

2) K. Fukui et al.: Jpn. J. Appl. Phys. **38** (1999) Suppl.38-1, 538.

3) K. Fukui, H. Nakagawa, I. Shimoyama, K. Nakagawa, H. Okamura, T. Nanba, M. Hasumoto and T. Kinoshita: J. Synchrotron Rad. **5** (1998) 836.

4) K. Fukui, H. Miura, H. Nakagawa, I. Shimoyama, K. Nakagawa, H. Okamura, T. Nanba, M. Hasumoto and T. Kinoshitato: Nucl. Instrum. & Methods in Phys. Res. A. (to be published).

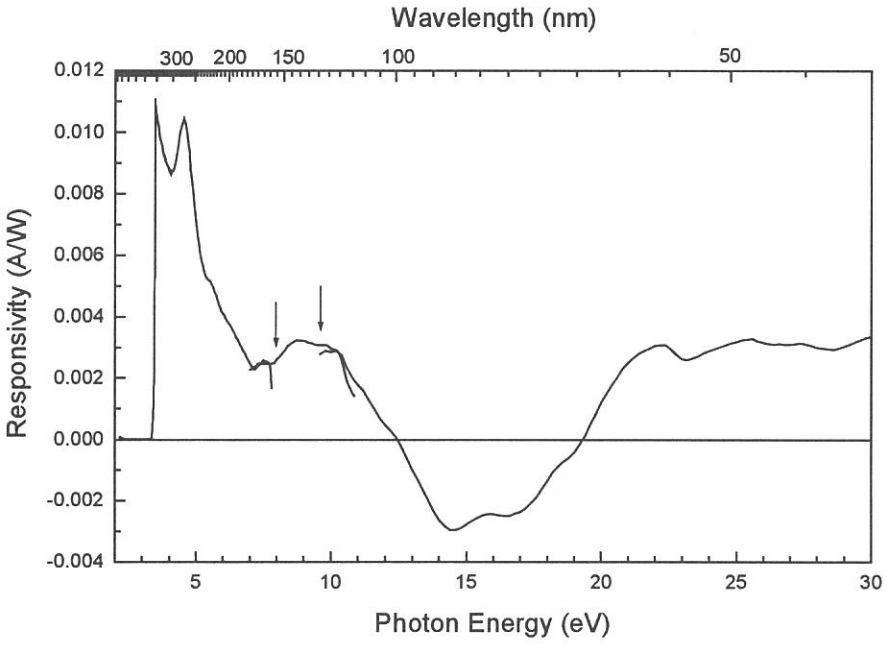

Fig.1. The responsivity spectra of GaN based Shottky type UV detector.

BL-7B

Vacuum Ultraviolet Absorption Spectra of Amino Acids (2): Tryptophan and Methionine

Kazumichi Nakagawa[A)] [1], Hiroyuki Arii[A)], *Yoko Kodama[B)], and **Masahito Tanaka[C)]

[A)]Faculty of Human Development, Kobe University, Tsurukabuto, Nada-Ku, Kobe 657-8501.
[B)]Graduate School of Cultural Studies and Human Sciences, Rokkodai, Nada-Ku, Kobe 657-8501.
[C)]Graduate school of Science and Technology, Tsurukabuto, Nada-Ku, Kobe 657-8501.

Although amino acids are known to be important building block of the life body, little is known about absorption spectra [2], because the main part of oscillator strength of these molecules is in the region of vacuum ultraviolet.

We measured absorption spectra of thin films of tryptophan (Trp) and methionine (Met) evaporated on collodion films. Thickness of amino acid films was estimated to be about 40 nm by a calibration with HPLC technique. Measurement was performed at the BL-7B in the wavelength region from 40 to 350 nm. In order to minimize the error in measurement of very weak transmitted light around 70 nm, we used an electron multiplier as a detector for 40 – 130 nm. Extremely low pressure of amino acid films allowed us measurement in vacuum at room temperature.

Obtained result was shown in Fig. 1.

The 220 nm peak of Trp was analyzed on the basis of peak position of the similar peaks of benzene (185 nm) and that of phenylalanine (198 nm) [2]. On the basis of this comparison, we tentatively concluded that the 220 nm peak of Trp was originated from the benzene ring part of Trp. The 280 nm peak of Trp was analyzed in comparison with absorption spectra of glycine, alanine and aspartic acid [2, 3]. This comparison showed that the 280 nm peak was found only for the case of Trp, which implies that the 280 nm peak was due to the pentagon part of Trp.

In order to confirm these assignments, we made a molecular orbital calculation using the WinMOPAC software. A tentative result showed that a transition due to benzene ring was found around 220 nm and that a transition due to the pentagon part was found around 280 nm. Other results of calculation were in a good harmony with the experimental results. Detailed analysis is being done.

References

[1] E-mail address is nakagawa@kobe-u.ac.jp .
[2] K. Nakagawa et al., in "The role of Radiation in the Origin and Evolution of Life", ed. By M. Akaboshi et al., Kyoto University Press, 2000, Kyoto, Japan, pp. 353-362.
[3] T. Inakagi, Biopolymers 12(1973)1353-1362.

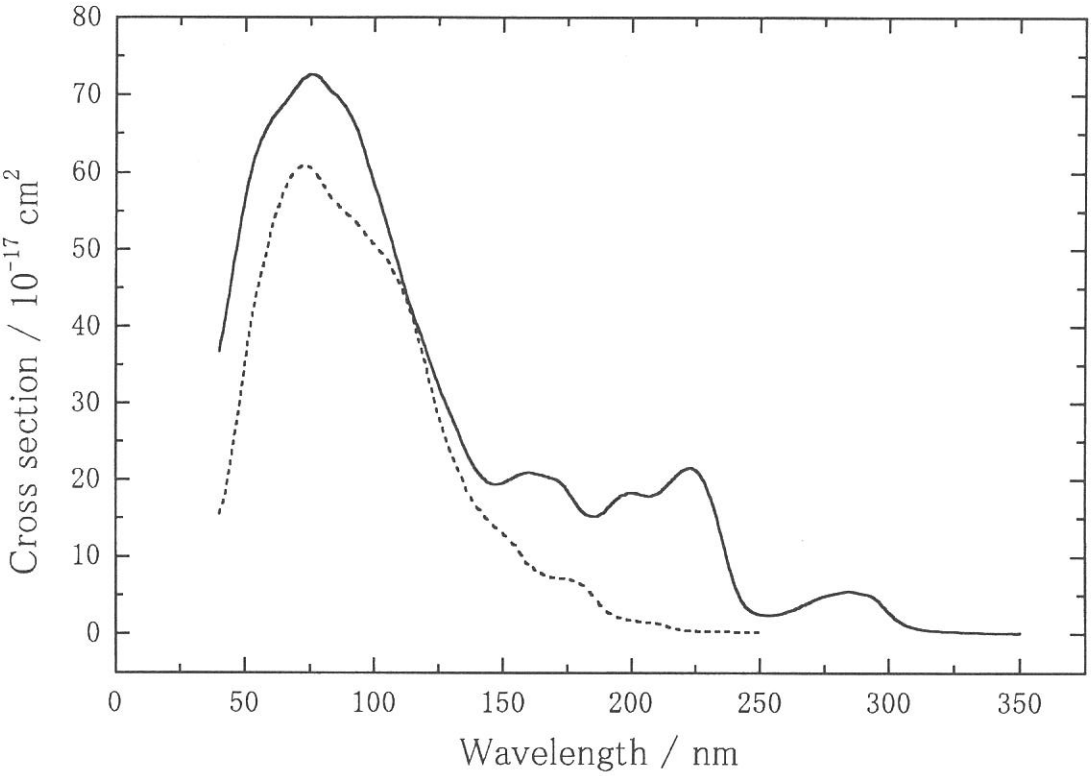

Fig.1. Absorption spectra of L-tryptophan (solid line) and L-methionine (dotted line).

(BL7B)

Luminescence and Reflectance Spectra of $CdBr_2$ Crystal

Kazutoshi FUKUI, Takayoshi Kihara[1], Hideyuki Nakagawa[1]

Institute for Molecular Science, Okazaki 444-8585, Japan

Fax +81-564-54-7079, fukui@fuee.fukui-u.ac.jp

[1] *Faculty of Engineering, Fukui University, Fukui 910-8507, Japan*

The cadmium bromide crystal ($CdBr_2$), which has indirect band gap, is an ionic layer compound. The crystal structure of $CdBr_2$ belongs to the rhombohedral $CdCl_2$ structure [1]. An Cd ion sheet is sandwiched by two I ion sheets and this basic layer stacks with each other. The crystal *c*-axis is perpendicular to these ion sheets. The bonding nature between Cd and Br ions is mainly ionic. However, that between adjacent Br ion sheets is of the Van der Waals force. In this report, we represent the visible – ultraviolet emission spectra, which are excited by the photon energy from near band edge to 30 eV, and their excitation spectra.

The experiments were carried out at BL7B. A single UV optical fiber cable, which was dedicated for ultra high vacuum (UHV) and had 0.6 mm core diameter, were used for detecting VIS and UV luminescence in the UHV chamber. VIS and UV luminescence lights were introduced to the VIS-UV monochromator with CCD array detector via both a UHV fiber optic feedthrough and a 5 m single optical fiber (0.6 mm core diameter). The $CdBr_2$ samples are single crystals, which are grown from the melt by the Stockbarger technique. The starting powder is commercially available $CdBr_2$ powder of 99.99% purity. The purification is carried out by the normal freezing method. The samples were cleaved just before the installation in the vacuum chamber. The incident light is parallel to the *c*-axis. The measurements were carried out in the range of 10^{-9} – 10^{-10} Torr from 15K to

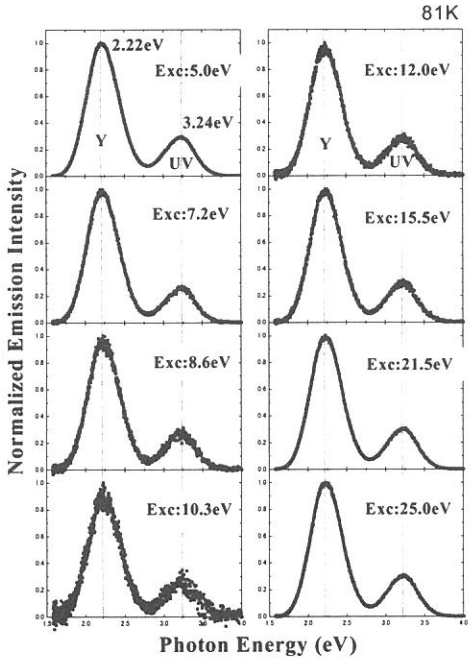

Fig.1 Emission spectra of CdBr2 at 81 K. The excitation energies are from 5.5.0 eV to 25.0 eV.

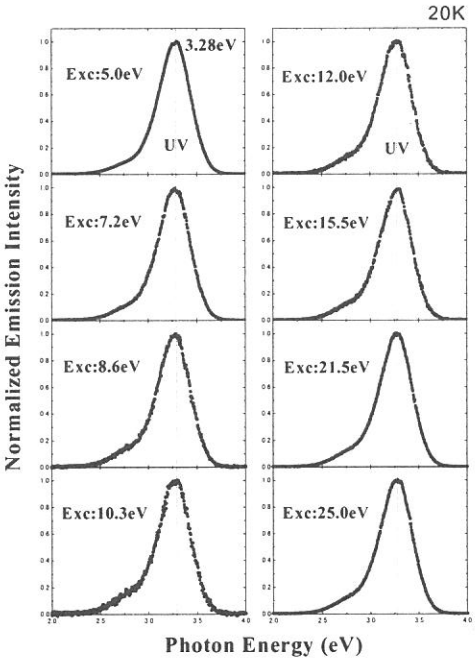

Fig.2 Emission spectra of CdBr2 at 20 K. The excitation energies are from 5.5.0 eV to 25.0 eV.

300 K.

Figure 1 shows the emission spectra at 81K. There are two emission bands. One is UV emission band at about 3.24 eV, the other Y emission band at around 2.22 eV. As shown in Fig. 2, the UV-emission becomes dominant emission band with decreasing temperature. These results are agreement with the previous precise work, which is carried out with D_2 lamp as the excitation light source [1]. The spectral distribution does not depend on the excitation energy from 5.0 to 25.0 eV. It means that the luminescence decay process does not change even though Cd 4*d* (and Br 4*s*) outermost inner core electrons are excited. It also suggests that the spectral distribution of the excitation spectra of both UV and Y emission bands are similar with each other.

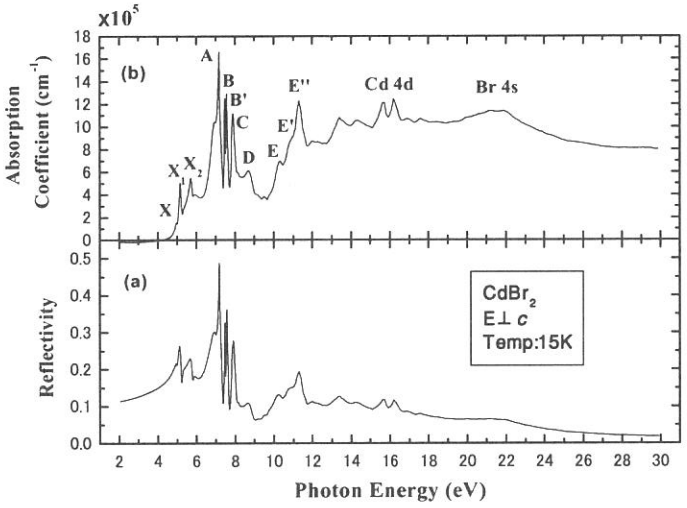

Fig.3 Reflectance spectrum of $CdBr_2$ at 20 K (a) and absorption spectrum (b) derived from (a) through the Kramers-Kronig analysis.

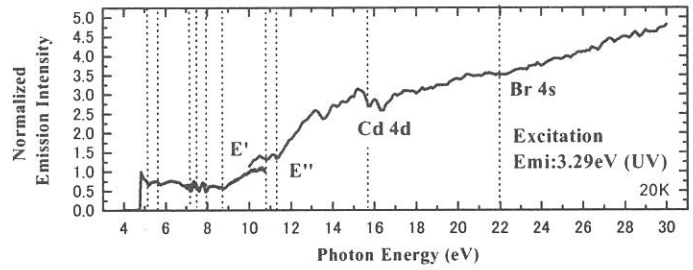

Fig.4 Excitation spectrum of the UV emission band of $CdBr_2$ at 20 K.

The reflectance spectrum at 20 K is shown in Fig. 3(a). Figure 3(b) shows the absorption spectrum derived from Fig. 3(a) through the Kramers-Kronig analysis. These results are agreement with the previous work [2]. The excitation spectrum of UV emission band at 20 K is shown in Fig. 4. The vertical lines indicate the location of the absorption peaks as shown in Fig. 3(b). The emission intensity is increasing with increasing photon energy. The UV emission starts at about 4.8 eV and the upsweep at around 11 eV is due to the transition to the upper conduction band. The dips correspond to the absorption peaks may due to the existence of the surface dead layer or of the other non-radiative decay channel such as photoelectron emission.

References

[1] H. Nakagawa and M. Kitaura, SPIE **2362** (1994) 295.

[2] M. Fujita, H. Nakagawa, H. Matsumoto, T. Miyanaga, M. Watanabe, K. Fukui, E. Ishiguro, Y. Fujii and Y. Sakisaka, J. Phys. Soc. Jpn. **59** (1990) 338.

(BL8B1)

Soft X-ray Excited Visible – Ultraviolet Emission Spectra of AlGaN Crystal

Kazutoshi FUKUI, Hideki HIRAYAMA [1], Satoru TANAKA[2] and Yoshinobu AOYAGI [1]

Institute for Molecular Science, Okazaki 444-8585, Japan

Fax +81-564-54-7079, fukui@fuee.fukui-u.ac.jp

[1] *Institute of Physical and Chemical Research (RIKEN), Wako 351-0198, Japan*

[2] *Research Institute for Electronic Science, Hokkaido University, Sapporo 060-0812, Japan*

The soft X-ray excited Visible (VIS) – Ultraviolet (UV) emission spectra (SXEVUES) of AlGaN have been measured. The emission spectra, which are excited by the band-to-band transition energy region, give us the information of luminescence decay process. SXEVUES gives us not only the excitation energy dependence but also the ion-site dependence of the luminescence decay process. Furthermore, both intensity and time correlation among the SXEVUES, the soft X-ray emission spectra (SXEA), and the photoelectron yield spectra will be interesting for the decay studies of the high photon energy excitation. In this report, we represent the first tentative results of SXEVUES of the wurtzite $Al_{1-x}Ga_xN$ (x= 0.14) and their temperature dependence.

The experiments were carried out at BL8B1. A single UV optical fiber cable, which was dedicated for ultra high vacuum (UHV) and had 0.6 mm core diameter, were used for detecting VIS and UV luminescence in the UHV chamber. VIS and UV luminescence lights were introduced to the VIS-UV monochromator with CCD array detector via both a UHV fiber optic feedthrough and a 5 m single optical fiber (0.6 mm core diameter). Thin film was made by the MOCVD method at RIKEN on SiC substrate. Sample was cleaned with organic solvents just before the installation in the vacuum chamber. No specific surface cleaning of the samples was performed in the vacuum chamber. The SXEVUES measurements were carried out in the range of 10^{-8} Torr from 25K to 200 K.

Figure 1 shows the VIS – UV region emission spectra of $Al_{0.14}Ga_{0.86}N$ thin film from 25K to 201K. The excitation energy is about 330 eV. The spectral distribution does not depend on the excitation energy around the nitrogen K edge (330 – 440 eV). There are at least three emission bands : first one around 3.75 eV (UV), second one around 2.3 eV (Y) and last one around 1.9 eV. According to the similarity of the first two bands in the emission spectrum to those of GaN [1], the first band consists of the exciton peaks, and the band at about 2.3 eV may be associated with deep levels. The deep levels arise due to the cation or nitrogen defects. Figure 2 shows the VIS – UV region emission spectra of SiC substrate from 25K to 208K. In case of SiC substrate, there are at least two emission bands. The first band is located at about 2.6 eV and the other is at about 1.9 eV. The 2.6 eV band on SiC substrate cannot be seen in Fig. 1, so that 3.75 eV and 2.3 eV bands in Fig. 1 are the original emission bands of $Al_{0.14}Ga_{0.86}N$ material. However, the similarity of the 1.9 eV band between Fig. 1 and 2 may suggest that both SiC and $Al_{0.14}Ga_{0.86}N$ surfaces are contaminated by the same material. It may be due to the high vacuum pressure and the surface sensitive character of the SXEVUES.

As shown in Fig. 1, the intensities of the UV and Y bands show the different temperature dependence behavior. The intensity of UV band decreases with increasing temperature even at 25K. However, Y band keeps

its intensity up to 53 K. It means that two bands have different potential barriers in the decay process. Further measurements and the combination with the near band-edge emission measurements will be held.

References

[1] S.C. Jain, M. Willander, R. Van Overstraeten, J. Appl. Phys. **87** (2000) 965.

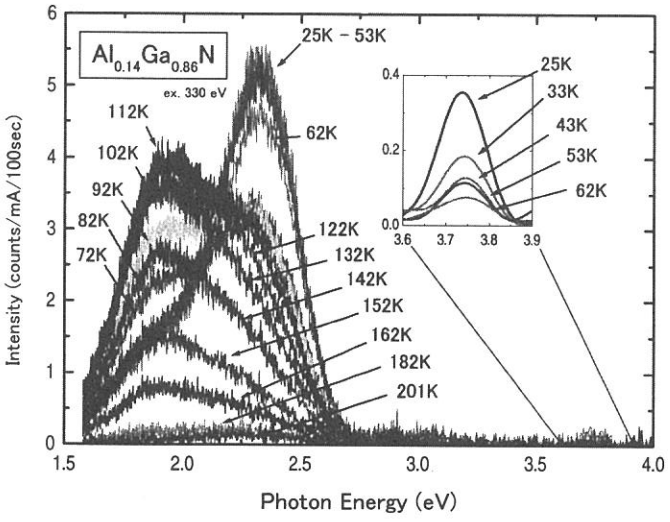

Fig.1 Emission spectra of $Al_{0.14}Ga_{0.86}N$ at various temperature. The excitation energy is 330 eV.

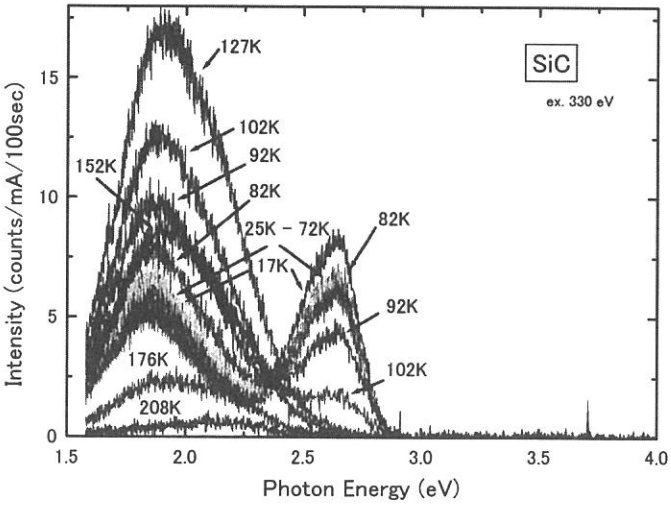

Fig.2 Emission spectra of SiC substrate at various temperature. The excitation energy is 330 eV.